iScience

CellPress
OPEN ACCESS

Article

Cholesterol Regulates Innate Immunity via Nuclear Hormone Receptor NHR-8

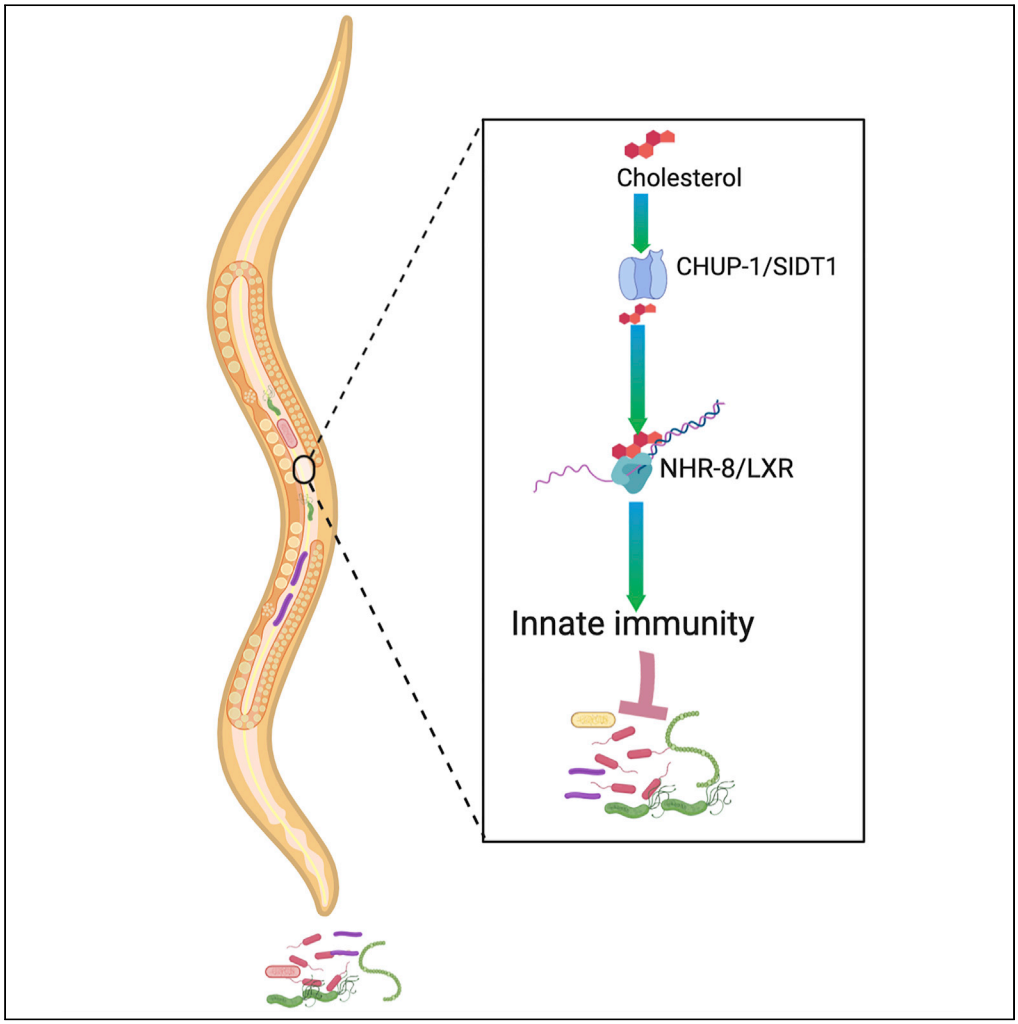

Benson Otarigho, Alejandro Aballay

aballay@ohsu.edu

HIGHLIGHTS

Cholesterol is required for *C. elegans* immunity against *P. aeruginosa* infection

Cholesterol is required during animal development for proper immunity and lifespan

CHUP-1 is required for the effect of cholesterol in defense against infection

Cholesterol acts through NHR-8 to transcriptionally regulate immune genes

DATA AND CODE AVAILABILITY

GSE136881
GSE137058

Otarigho & Aballay, iScience *23*, 101068
May 22, 2020
https://doi.org/10.1016/j.isci.2020.101068

iScience

CellPress
OPEN ACCESS

Article

Cholesterol Regulates Innate Immunity via Nuclear Hormone Receptor NHR-8

Benson Otarigho[1] and Alejandro Aballay[1,2,*]

SUMMARY

Cholesterol is an essential nutrient for the function of diverse biological processes and for steroid biosynthesis across metazoans. However, the role of cholesterol in immune function remains understudied. Using the nematode *Caenorhabditis elegans*, which depends on the external environment for cholesterol, we studied the relationship between cholesterol and innate immunity. We found that the transporter CHUP-1 is required for the effect of cholesterol in the development of innate immunity and that the cholesterol-mediated immune response requires the nuclear hormone receptor NHR-8. Cholesterol acts through NHR-8 to transcriptionally regulate immune genes that are controlled by conserved immune pathways, including a p38/PMK-1 MAPK pathway, a DAF-2/DAF-16 insulin pathway, and an Nrf/SKN-1 pathway. Our results indicate that cholesterol plays a key role in the activation of conserved microbicidal pathways that are essential for survival against bacterial infections.

INTRODUCTION

Cholesterol is an important nutrient and precursor for bile, vitamin D, oxysterols, and steroid hormones (Magner et al., 2013; Prabhu et al., 2016). In addition, it plays an important role in diverse biological processes, including metabolism, membrane structure, and cell signaling (Ihara et al., 2017; Kawasaki et al., 2013; Magner et al., 2013; Shanmugam et al., 2017), and has been implicated in the regulation of lifespan and aging (Chen et al., 2019; Cheong et al., 2011, 2013; Ihara et al., 2017; Lee et al., 2005, 2007; Lee and Schroeder, 2012; Magner et al., 2013; Shanmugam et al., 2017). Despite this wealth of information about cholesterol's functions, there is little information about its role in the immune system, which is essential for defense against invading pathogens.

Vertebrates have a functional mevalonate pathway that is involved in the synthesis of cholesterol and other useful lipids that are synthesized from acetyl-CoA through the activity of the 3-hydroxy-3-methyl-glutaryl-coenzyme A reductase (Sapir et al., 2014). Although the mevalonate pathway is evolutionarily conserved in the nematode *Caenorhabditis elegans*, the animal lacks this reductase (Rauthan and Pilon, 2011). Thus, *C. elegans* depends on the external environment for cholesterol or other sterol supplements (Chitwood and Lusby, 1991; Hieb and Rothstein, 1968; Shanmugam et al., 2017). The possibility of tightly controlling cholesterol concentrations has facilitated the use of *C. elegans* to study cholesterol and lipid homeostasis to answer critical biological questions about health and longevity (Cheong et al., 2011, 2013; Ihara et al., 2017; Magner et al., 2013; Shanmugam et al., 2017).

C. elegans imports cholesterol via conserved cholesterol transporters, such as CHUP-1 (cholesterol uptake associated) (Méndez-Acevedo et al., 2017; Valdes et al., 2012; Whangbo et al., 2017), NPC1 (Ikonen, 2008; Rosenbaum et al., 2009; Smith and Levitan, 2007), and other related proteins (Brown et al., 2008; Chen et al., 2016, 2019; Zhang et al., 2017). At the cellular level, different nuclear hormone receptors (NHRs), such as NHR-8, NHR-25, NHR-48, NHR-49, and NHR-80, bind and/or regulate cholesterol, lipids, hormone homeostasis, and metabolism in *C. elegans* (Antebi, 2006). In addition to their role in the coordination of metabolism, NHRs play key functions in the control of development, reproduction, and homeostasis (Bodofsky et al., 2017; Houthoofd et al., 2002; Piskacek et al., 2019; Ratnappan et al., 2016; Wang et al., 2015).

Here we investigated the relationship between cholesterol and innate immune defense in *C. elegans*. We found that cholesterol is required for proper development of immune defense against infection by the pathogen *Pseudomonas aeruginosa* and that the transporter CHUP-1 is required for the function of

[1]Department of Molecular Microbiology & Immunology, Oregon Health & Science University, Portland, OR 97239, USA

[2]Lead Contact

*Correspondence: aballay@ohsu.edu

https://doi.org/10.1016/j.isci.2020.101068

cholesterol in immunity. We also found that the cholesterol-mediated immune response requires NHR-8 to transcriptionally regulate immune genes that are controlled by conserved immune pathways, including a p38/PMK-1 MAPK pathway, a DAF-2/DAF-16 insulin pathway, and an Nrf/SKN-1 pathway. Our findings indicate that the innate immune system requires cholesterol to engage an NHR-8 immune pathway that primarily controls PMK-1 and is essential for host immune defense against pathogens.

RESULTS

Cholesterol Is Required for *C. elegans* Defense against *P. aeruginosa* Infection

To study the role of cholesterol in innate immunity, we performed infections with the pathogen *P. aeruginosa* using wild-type *C. elegans* previously grown on lawns of *E. coli* in the absence of cholesterol supplementation; with 5 μg/mL cholesterol, which is the standard laboratory concentration to propagate the nematodes; and with 20 μg/mL cholesterol. Because strict sterol-free conditions affect the development of the animal, reduce the brood size, and result in dauer formation in the second generation (Matyash et al., 2004; Merris et al., 2003), in our studies we used conventional nematode growth media, which contains sufficient sterols to support *C. elegans* development. As shown in Figure S1, the absence or presence of cholesterol supplementation did not change the brood size or the development of the animals. To further address whether the absence of cholesterol supplementation affects the development of the animal, we used the GR1452 strain, which is a reporter of gene *col-19* that is sharply expressed at the late L4/young adult transition (Hayes et al., 2011). The absence of cholesterol supplementation did not affect the expression of GFP driven by the promoter of *col-19*, suggesting that the development of the animals under different cholesterol concentrations is similar (Figure S1C-D). Although GFP could accumulate over time and the results might vary when looked at specific time points before and after the molting, we did not observe any delay in the development of the animals into young adults (Figure S1A), which were used in our survival studies. We found that young adult animals grown in the absence of cholesterol supplementation were more susceptible to *P. aeruginosa*-mediated killing than animals grown in the presence of 5 μg/mL cholesterol (referred to as control cholesterol) (Figure 1A). In contrast, animals grown on plates containing 20 μg/mL cholesterol (referred to as high cholesterol) were more resistant to pathogen infection than animals grown on control plates (Figure 1A), indicating that cholesterol was required for *C. elegans* defense against *P. aeruginosa* infection.

To address the possibility that the absence of cholesterol supplementation might reduce the virulence of *P. aeruginosa*, we only changed the cholesterol concentrations prior to infection. As shown in Figure 1B, the presence or absence of cholesterol supplementation before infection affected the susceptibility of the animals to *P. aeruginosa*. Consistent with the idea that cholesterol acts on the host immune system rather than on *P. aeruginosa* virulence, there was no significant difference in the susceptibility of animals grown on standard cholesterol concentrations and animals infected with *P. aeruginosa* grown on different cholesterol concentrations (Figure 1C). The effect of cholesterol-mediated immune defense on *P. aeruginosa* bacterial colonization was examined by visualizing bacteria expressing GFP and quantifying the number of bacterial cells in the intestine of the animals. Although the absence of cholesterol supplementation had no effect on bacterial burden, high cholesterol significantly reduced it (Figures 1D and 1E). Taken together, our findings indicate that cholesterol is required during the development of *C. elegans* for proper resistance against *P. aeruginosa* infection.

Because several studies have indicated that cholesterol is critical for *C. elegans* lifespan (Cheong et al., 2011, 2013; Ihara et al., 2017; Lee et al., 2005; Lee and Schroeder, 2012; Magner et al., 2013; Shanmugam et al., 2017), we studied the effect of different cholesterol concentrations on the survival of animals grown on control *E. coli*. Although animals grown in the absence of cholesterol supplementation exhibited a shorter lifespan, those grown on high cholesterol exhibited a longer lifespan than control animals (Figure S2A). Because *E. coli* proliferation is a cause of death in *C. elegans* (Garigan et al., 2002; Sutphin and Kaeberlein, 2009) and animals deficient in the immune response are persistently colonized and killed by *E. coli* (Kerry et al., 2006; Singh and Aballay, 2006; Tenor and Aballay, 2008), we examined the effect of cholesterol on the lifespan of animals on lawns of heat-killed *E. coli*. The survival of animals grown in the absence of cholesterol supplementation was not significantly different from that of control animals, indicating that the absence of cholesterol supplementation did not significantly affect lifespan. In contrast, the animals that were grown on high cholesterol had a slightly longer lifespan than the control animals (Figure S2B). These findings indicate that cholesterol is required for defense against infection and that cholesterol supplementation during animal development may not only boost the immune response but also improve the lifespan of the animals.

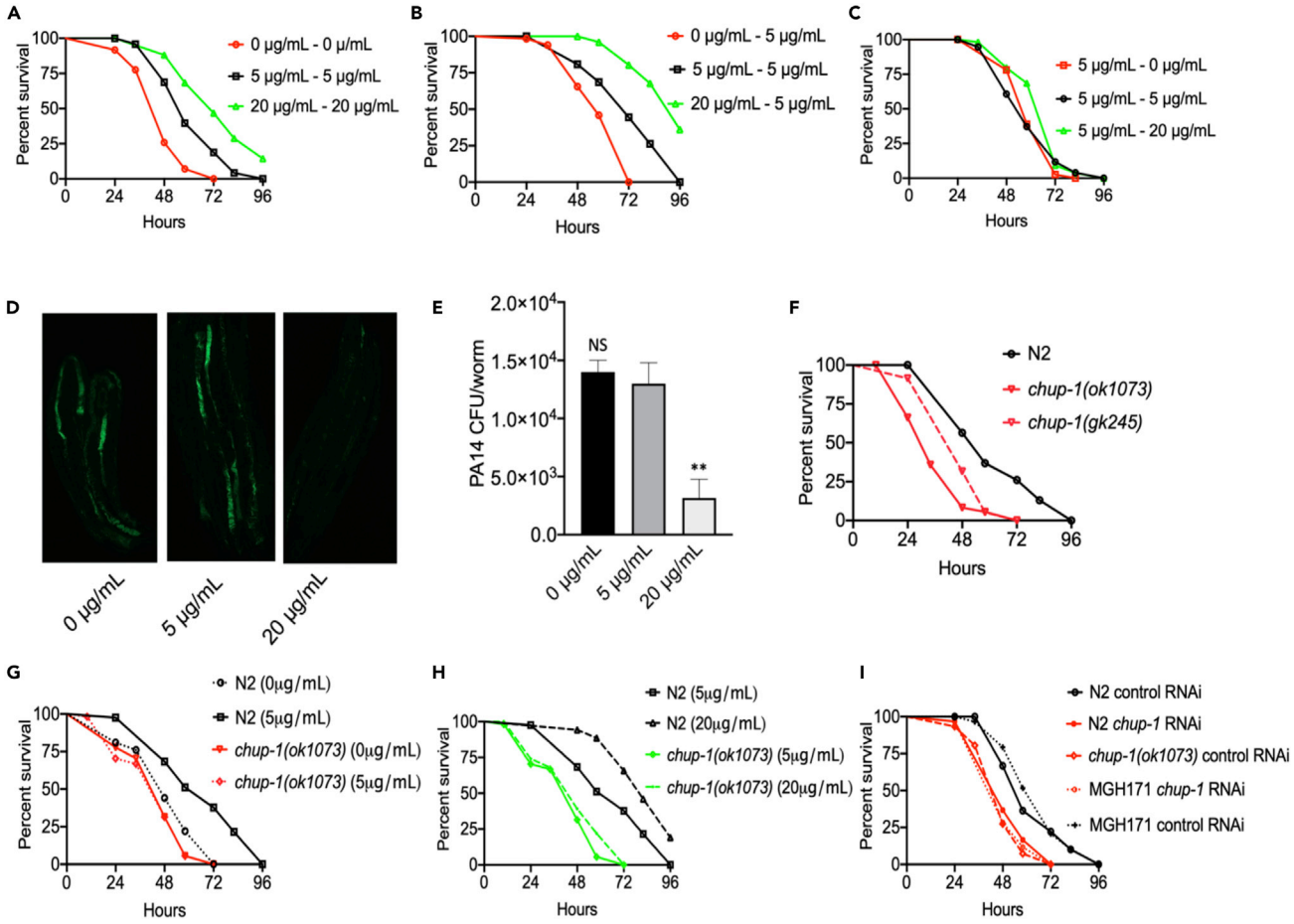

Figure 1. Cholesterol Is Required for *C. elegans* Resistance against *P. aeruginosa*

(A) Wild-type animals were grown in the absence of cholesterol supplementation (0 µg/mL) or at different cholesterol concentrations, exposed to *P. aeruginosa* cultured on the same cholesterol concentrations, and scored for survival. WT animals grown on 5 µg/mL cholesterol (control) versus 0 µg/mL, $P < 0.0001$; 20 µg/mL, $P < 0.0001$.

(B) WT animals were grown on different cholesterol concentrations, exposed to *P. aeruginosa* cultured at the control cholesterol concentration (5 µg/mL) and scored for survival. WT animals grown on 5 µg/mL cholesterol (control) versus 0 µg/mL, $P < 0.0001$; 20 µg/mL, $P < 0.0001$.

(C) WT animals were grown on control cholesterol concentration (5 µg/mL), exposed to *P. aeruginosa* cultured on different cholesterol concentrations (0, 5 and 20 µg/mL) and scored for survival. WT animals grown on 5 µg/mL cholesterol (control) versus 0 µg/mL, P = NS; 20 µg/mL, P = NS.

(D) WT animal colonization by *P. aeruginosa*-GFP after 24 h at 25°C.

(E) Colony-forming units per animal grown on *P. aeruginosa* -GFP after 24 h at 25°C. Bars represent means, whereas error bars indicate SD; $^{**}p < 0.05$, NS = not significant.

(F) *chup-1(ok1073)* mutants were grown on 5 µg/mL cholesterol (control), exposed to *P. aeruginosa*, and scored for survival. WT animals versus *chup-1(ok1073)* and *chup-1(gk245)*, $P < 0.0001$.

(G) *chup-1(ok1073)* mutants were grown on 0 and 5 µg/mL cholesterol, exposed to *P. aeruginosa*, and scored for survival. WT animals grown on 5 µg/mL cholesterol (control) versus 0 µg/mL, $P < 0.0001$; *chup-1(ok1073)*, $P < 0.0001$.

(H) *chup-1(ok1073)* mutants were grown on 20 and 5 µg/mL cholesterol, exposed to *P. aeruginosa*, and scored for survival. WT animals grown on 5 µg/mL cholesterol (control) versus 20 µg/mL, $P < 0.0001$; *chup-1(ok1073)* 20 µg/mL, $P < 0.0001$; *chup-1(ok1073)* 5 µg/mL, $P < 0.0001$.

(I) Control, MGH171(*chup-1* RNAi), WT (*chup-1* RNAi) animals were grown on 5 µg/mL cholesterol, exposed to *P. aeruginosa*, and scored for survival. WT on control RNAi versus *chup-1(ok1073)* control RNAi, $P < 0.0001$; WT *chup-1* RNAi, $P < 0.0001$; MGH171 *chup-1* RNAi, $P < 0.0001$; MGH171 control RNAi, P = NS.

C. elegans is auxotrophic for cholesterol (Chitwood and Lusby, 1991; Hieb and Rothstein, 1968) and requires different proteins to bind and transport cholesterol (Brown et al., 2008; Chen et al., 2016, 2019; Huber et al., 2006; Kamal et al., 2019; Méndez-Acevedo et al., 2017; Ranawade et al., 2018; Sym et al., 2000; Valdes et al., 2012; Zhang et al., 2017). Thus, we investigated the roles of different transporters in the cholesterol-mediated immune response by exposing loss-of-function mutants in genes known to encode cholesterol transporters to *P. aeruginosa*. We found that animals carrying deletions in genes *chup-1* and *sms-5* showed enhanced susceptibility to *P. aeruginosa*-mediated killing at control cholesterol

concentrations (Figures 1F, 1G, and S3). However, only *chup-1* mutation suppressed the enhanced resistance to *P. aeruginosa*-mediated killing induced by high cholesterol (Figure 1H), suggesting that CHUP-1 is the only required transporter for the effect of high cholesterol supplementation on pathogen resistance. The intestinal contribution of CHUP-1 in cholesterol-mediated defense was examined by utilizing a *C. elegans* strain capable of RNAi activity only in the intestine (strain MGH171), in which RNAi knockdown of CHUP-1 completely suppressed the effect of high cholesterol on *C. elegans* resistance to *P. aeruginosa* infection (Figures 1I, S3C, and S3D). These results suggest that CHUP-1 is required in the intestine to mediate the effect of cholesterol on pathogen resistance.

Transcriptomics Identification of Cholesterol-Dependent Immune Genes

To gain insights into the host defense mechanisms that require cholesterol to combat bacterial infections, we performed transcriptomics analyses to identify genes that were upregulated in animals grown on high cholesterol or downregulated in animals grown in the absence of cholesterol supplementation relative to animals grown on the control cholesterol concentration (Table S1). Overall, the gene expression data showed an important overlap between genes that were upregulated by high cholesterol and those that were downregulated in the absence of cholesterol supplementation (Figure 2A). To identify related gene groups that were responsible for the effect of cholesterol on resistance to *P. aeruginosa* infection, we employed an unbiased gene enrichment analysis using the database for annotation, visualization, and integrated discovery (DAVID, http://david.abcc.ncifcrf.gov) (Dennis et al., 2003) (Table S2). The 10 Gene Ontology (GO) clusters with the highest DAVID enrichment score for a number of vital biological functions are shown in Figure 2B. For the subset of genes that were upregulated in animals grown on high cholesterol or downregulated in animals grown in the absence of cholesterol supplementation, the metabolic process cluster was the most highly enriched, followed by the innate immune/defense cluster (Figure 2B and Table S3). As expected, a similar enrichment was also observed using a Wormbase enrichment analysis tool (https://wormbase.org/tools/enrichment/tea/tea.cgi) (Angeles-Albores et al., 2016, 2018) that is specific for *C. elegans* gene data analyses (Figures S4A and S4B). Metabolic and immune genes were also highly enriched among the 1,449 genes that overlapped (Figures 2C and S4B).

We used WormExp (http://wormexp.zoologie.uni-kiel.de/wormexp/) (Yang et al., 2016), which integrates all published expression data for *C. elegans*, to analyze the two most highly enriched GO clusters. The further analysis of the metabolic cluster revealed a number of genes that are differentially expressed during development (Table S4), which suggest that, even though animals fed different cholesterol concentrations seem to reach adulthood at the same time (Figure S1A), there may be small differences during larval development among the different populations used in this study. The study of the immune cluster indicated that genes controlled by a p38/PMK-1 MAPK pathway were the most highly overrepresented among those upregulated by high cholesterol or downregulated by the absence of cholesterol supplementation (Tables S4 and S5). Other pathways involved in *C. elegans* innate immunity, including a DAF-2/DAF-16 insulin pathway and a Nrf/SKN-1, were also enriched (Figure 2D and Table S5). Several of the SKN-1-, ELT-2-, DAF-16-dependent genes are also controlled by PMK-1 (Tables S4 and S5), indicating that the PMK-1 pathway is a main pathway by which high cholesterol promotes innate immunity. The activation of PMK-1 by high cholesterol was confirmed by directly measuring the levels of active PMK-1 (Figure S4C). Taken together, these results indicate that cholesterol enhances *C. elegans* resistance to *P. aeruginosa* mainly by activating immune genes, several of which are controlled by the PMK-1 immune pathway.

We hypothesized that the enhanced resistance to *P. aeruginosa* infection of animals grown on high cholesterol might be due to the upregulation of immune genes. To test this hypothesis, we studied the role of suppression by mutation or RNAi of the immune pathways transcriptionally regulated by cholesterol. As shown in Figures 2E–2G, inactivation of *pmk-1*, *daf-16,* and *skn-1* completely or partially suppressed the enhanced resistance to *P. aeruginosa* induced by high cholesterol. Inhibition of *pmk-1* or *daf-16* did not enhance the effect of the absence of cholesterol supplementation (Figures S5A and S5B), further confirming that the cholesterol effect on animal survival following *P. aeruginosa* infection was due to the regulation of immune pathways. To address whether additional genes crucial for immunity are generally required for the beneficial effects of high cholesterol on defense against infection, we used *kgb-1* and *dbl-1* mutants, which have been shown to be susceptible to *P. aeruginosa* infection (Evans et al., 2008; Mallo et al., 2002; Pellegrino et al., 2014). Even though these animals are susceptible to *P. aeruginosa*-mediated killing, high cholesterol was able to improve their survival (Figures S5C–S5F). Consistent with the observed gene enrichment in PMK-1-dependent genes, these results indicate that PMK-1, and partially DAF-16 and SKN-1, are required for the immune activation caused by the presence of high cholesterol.

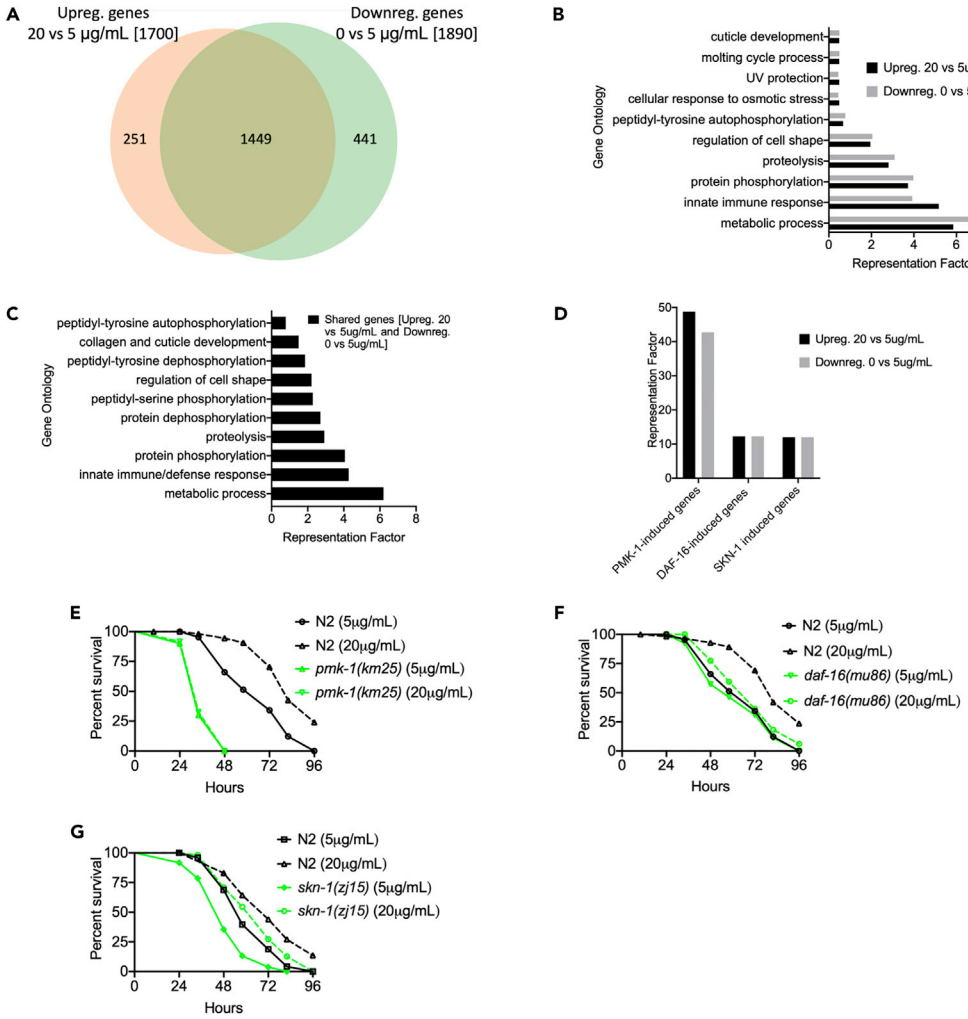

Figure 2. Cholesterol-Mediated Immunity Primarily Acts through a p38/PMK-1 MAPK Pathway

(A) Venn diagram showing upregulated genes (20 versus 5 µg/mL cholesterol) and downregulated genes (0 versus 5 µg/mL cholesterol).

(B) Gene ontology analysis of upregulated and downregulated genes in animals grown on 20 and 0 µg/mL cholesterol, respectively. The cutoff is based on the filtering thresholds of $P < 0.05$ and arranged according to the representation factor.

(C) Gene ontology analysis of shared genes between animals grown at 20 versus 5 µg/mL and 0 versus 5 µg/mL cholesterol. The cutoff is based on the filtering thresholds of $P < 0.05$ and arranged according to representation factor.

(D) Representation factors of immune pathways for the upregulated and downregulated immune genes in animals grown at 20 versus 5 and 0 versus 5 µg/mL cholesterol, respectively.

(E) WT and *pmk-1(km25)* animals were grown on 20 and 5 µg/mL cholesterol, exposed to *P. aeruginosa*, and scored for survival. WT animals grown on 5 µg/mL cholesterol (control) versus 20 µg/mL, $P < 0.0001$; *pmk-1(km25)* 5 µg/mL, $P < 0.0001$; *pmk-1(km25)* 20 µg/mL, $P > 0.0001$. *pmk-1(km25)* 0 µg/mL versus *pmk-1(km25)* 5 µg/mL, P = NS.

(F) WT and *daf-16(mu86)* animals were grown on 20 and 5 µg/mL cholesterol, exposed to *P. aeruginosa*, and scored for survival. WT animals grown on 5 µg/mL cholesterol (control) versus 20 µg/mL, $P < 0.0001$; *daf-16(mu86)* 20 µg/mL, P = NS; *daf-16(mu86)* 5 µg/mL, P = NS.

(G) WT and *skn-1(zj15)* animals were grown on 20 and 5 µg/mL cholesterol, exposed to *P. aeruginosa*, and scored for survival. *skn-1(zj15)* animals grown on 5 µg/mL cholesterol (control) versus 20 µg/mL, $P < 0.001$.

Cholesterol Functions through NHR-8/PMK-1 to Promote Innate Immunity

Because cholesterol is a required precursor for the steroid biosynthesis pathway, which is evolutionarily conserved from *C. elegans* to mammals (Antebi, 2015; Calkin and Tontonoz, 2012; Fischer et al., 2013; Mooijaart et al., 2005; Rauthan and Pilon, 2011; Shanmugam et al., 2017; Watts and Ristow, 2017; Wollam

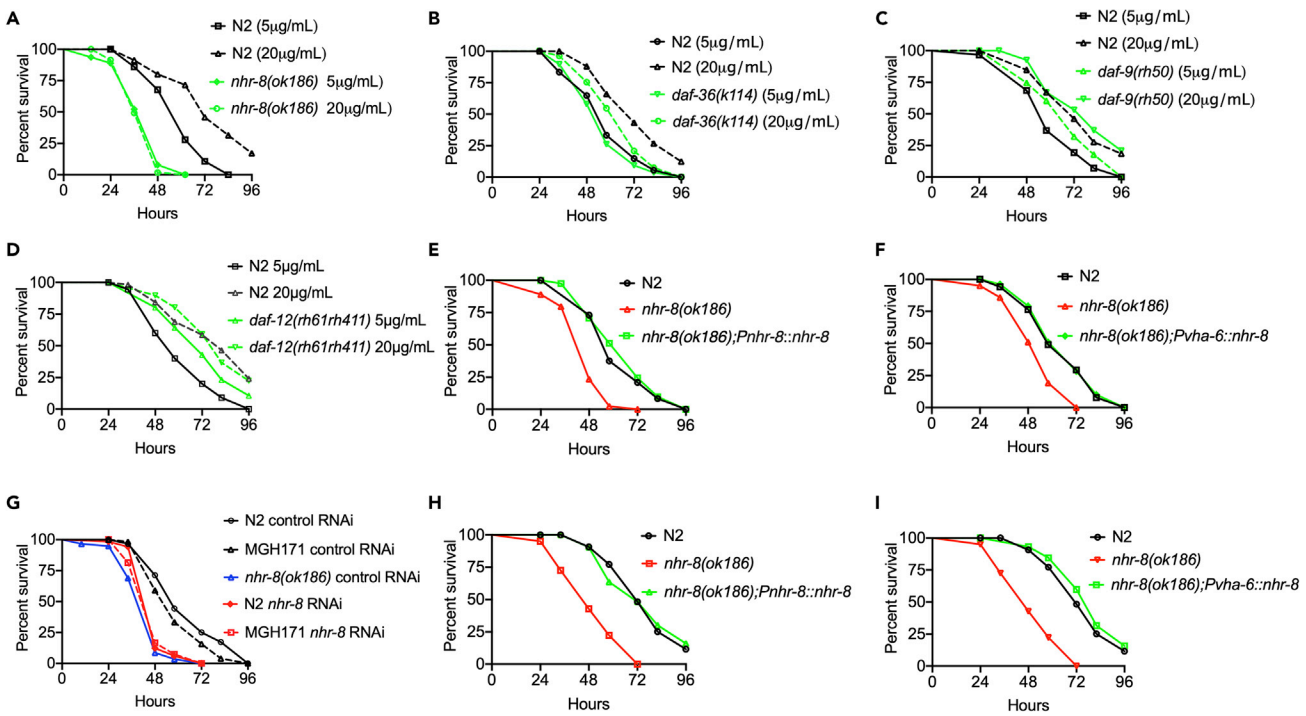

Figure 3. The Nuclear Hormone Receptor NHR-8 Mediates the Cholesterol Effect on the Immune System

(A) WT and *nhr-8(ok186)* animals were grown on 20 and 5 μg/mL cholesterol, exposed to *P. aeruginosa*, and scored for survival. WT animals grown on 5 μg/mL cholesterol (control) versus WT animals 20 μg/mL, $P < 0.0001$; *nhr-8(ok186)* 20 μg/mL, $P < 0.0001$; *nhr-8(ok186)* 5 μg/mL, $P < 0.0001$. *nhr-8(ok186)* mutant on 20 μg/mL versus *nhr-8(ok186)* 5 μg/mL, P = NS.

(B) WT and *daf-36(k114)* animals were grown on 20 and 5 μg/mL cholesterol, exposed to *P. aeruginosa*, and scored for survival. WT animals grown on 5 μg/mL cholesterol (control) versus WT animals 20 μg/mL, $P < 0.0001$; *daf-36(k114)* 20 μg/mL, $P < 0.0001$; *daf-36(k114)* 5 μg/mL, $P < 0.0001$. *daf-36(k114)* animals on 20 μg/mL versus *daf-36(k114)* 5 μg/mL, $P < 0.0001$.

(C) WT and *daf-9(rh50)* animals were grown on 20 and 5 μg/mL cholesterol, exposed to *P. aeruginosa*, and scored for survival. WT animals grown on 5 μg/mL cholesterol (control) versus WT animals 20 μg/mL, $P < 0.0001$; *daf-9(rh50)* 20 μg/mL, $P < 0.0001$; *daf-9(rh50)* 5 μg/mL, $P < 0.0001$. *daf-9(rh50)* animals on 20 μg/mL versus *daf-9(rh50)* 5 μg/mL, $P < 0.0001$.

(D) WT and *daf-12(rh61rh411)* animals were grown on 20 and 5 μg/mL cholesterol, exposed to *P. aeruginosa*, and scored for survival. WT animals grown on 5 μg/mL cholesterol (control) versus WT animals 20 μg/mL, $P < 0.0001$; *daf-12(rh61rh411)* 20 μg/mL, $P < 0.0001$; *daf-12(rh61rh411)* 5 μg/mL, $P < 0.0001$. *daf-12(rh61rh411)* animals on 20 μg/mL versus *daf-12(rh61rh411)* 5 μg/mL, $P < 0.0001$.

(E) WT, *nhr-8(ok186)*, and *nhr-8(ok186);Pnhr-8::nhr-8* animals were grown on 5 μg/mL cholesterol, exposed to *P. aeruginosa*, and scored for survival. WT animals versus *nhr-8(ok186)*, $P < 0.0001$; *nhr-8(ok186);Pnhr-8::nhr-8*, P = NS.

(F) WT, *nhr-8(ok186)*, and *nhr-8(ok186);Pvha-6::nhr-8* animals were grown on 5 μg/mL cholesterol, exposed to *P. aeruginosa*, and scored for survival. WT animals versus *nhr-8(ok186)*, $P < 0.0001$; *nhr-8(ok186);Pvha-6::nhr-8*, P = NS.

(G) Control, *nhr-8* RNAi WT and MGH171 animals were grown on 5 μg/mL cholesterol, exposed to *P. aeruginosa*, and scored for survival. WT control RNAi versus MGH171 *nhr-8* RNAi, $P < 0.0001$.

(H) WT, *nhr-8(ok186)*, and *nhr-8(ok186);Pnhr-8::nhr-8* animals were grown on 20 μg/mL cholesterol, exposed to *P. aeruginosa*, and scored for survival. WT animals versus *nhr-8(ok186)*, $P < 0.0001$; *nhr-8(ok186);Pnhr-8::nhr-8*, P = NS.

(I) WT, *nhr-8(ok186)*, and *nhr-8(ok186);Pvha-6::nhr-8* animals were grown on 20 μg/mL cholesterol, exposed to *P. aeruginosa*, and scored for survival. WT animals versus *nhr-8(ok186)*, $P < 0.0001$; *nhr-8(ok186);Pvha-6::nhr-8*, P = NS.

et al., 2011; Yoshiyama-Yanagawa et al., 2011), we reasoned that cholesterol-derived steroids might be required for proper function of the innate immune system. *C. elegans* NHR-8 regulates a steroid biosynthesis pathway (Figure S6) that has been linked to the control of cholesterol balance, fatty acid desaturation, apolipoprotein production, bile acid metabolism, and xenobiotic metabolism (Chow et al., 2014; Lindblom and Dodd, 2006; Magner et al., 2013; Ménez et al., 2019; Schindler et al., 2014). Thus, we studied the susceptibility to *P. aeruginosa*-mediated killing of mutants in the known NHR-8 steroid biosynthesis pathways and found that only *nhr-8* mutant animals were more susceptible to *P. aeruginosa* compared with wild-type animals (Figures S7A–S7F). In addition, *nhr-8(ok186)* fully suppressed the beneficial effect of high cholesterol (Figure 3A). Similar results were obtained using the *nhr-8(tm1800)* null allele (Figure S7B). Unlike mutations in *nhr-8*, mutations in *daf-36*, *daf-9*, and *daf-12* did not result in enhanced

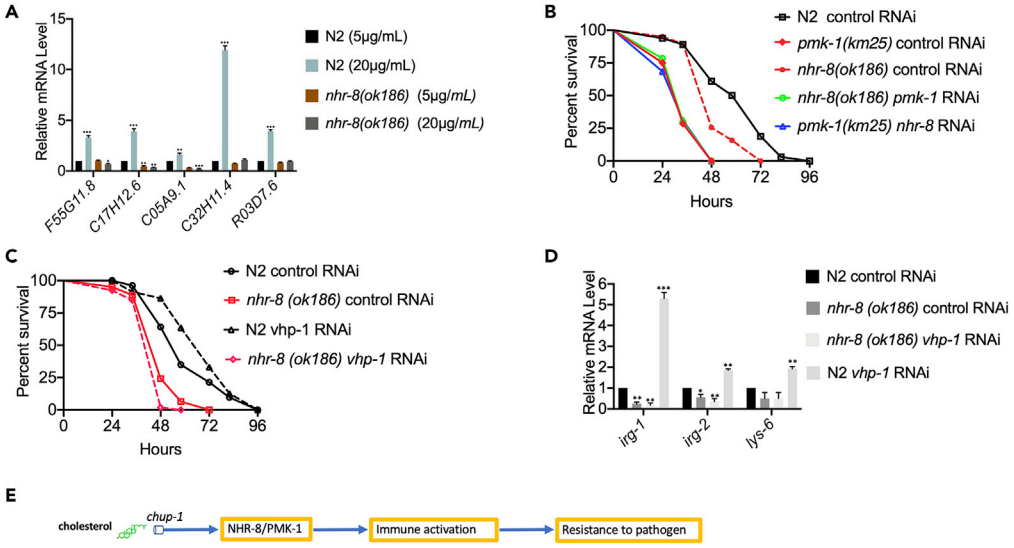

Figure 4. Cholesterol Activates the NHR-8/PMK-1 Immune Pathway

(A) Expression of cholesterol-mediated immune genes in WT and *nhr-8(ok186)* animals grown on 5 and 20 μg/mL cholesterol. *pmk-1*- (*F55G11.8, C17H12.6, C05A9.1, C32H11.4* and *R03D7.6*) and *daf-16*-dependent genes (*F55G11.8, C05A9.1*) were studied. Bars represent means, whereas error bars indicate SD; *p < 0.05, **p < 0.001 and ***p < 0.0001.

(B) Control, *pmk-1(km25)*, *nhr-8(ok186)*, and WT treated with *pmk-1* RNAi and *nhr-8* RNAi were grown on 5 μg/mL cholesterol, exposed to *P. aeruginosa*, and scored for survival. WT animals control RNAi versus *pmk-1(km25)* control RNAi, P < 0.0001; *nhr-8(ok186)* control RNAi, P < 0.001; WT *pmk-1* RNAi, P < 0.0001; WT *nhr-8* RNAi, P < 0.0001; *nhr-8(ok186) pmk-1* RNAi, P < 0.0001.

(C) Control, *nhr-8(ok186)*, and *vhp-1* RNAi were grown on 5 μg/mL cholesterol, exposed to *P. aeruginosa*, and scored for survival. WT animal versus *nhr-8(ok186)*, P < 0.001; *nhr-8(ok186) vhp-1* RNAi, P < 0.0001; N2 *vhp-1* RNAi, P < 0.001.

(D) Gene expression of *nhr-8(ok186)* and WT animals with control or *vhp-1* RNAi grown on 5 μg/mL cholesterol. Bars represent means, whereas error bars indicate SD; *p < 0.05, **p < 0.001, and ***p < 0.0001.

(E) Model for activation of the NHR-8/PMK-1/p38 MAPK immune pathway by cholesterol.

susceptibility to *P. aeruginosa* infection under high or control cholesterol concentrations (Figures 3B–3D), indicating that they are not part of the cholesterol-induced NHR-8/PMK-1 pathway that promotes innate immunity.

Expression of *nhr-8* under the control of its own promoter fully rescued the mutant phenotype of *nhr-8(ok186)* (Figure 3E). Consistent with its function in the intestine, NHR-8 expression under the regulation of the intestine-specific promoter *Pvhp-6* also fully rescued the mutant phenotype of *nhr-8(ok186)* animals (Figure 3F). The intestinal function of NHR-8 in immunity was further confirmed using strain MGH171, which allows intestine-specific RNAi (Figure 3G). Expression of *nhr-8* under the control of its own promoter or *Pvhp-6* fully rescued the enhanced susceptibility to *P. aeruginosa* of *nhr-8(ok186)* animals grown on a high cholesterol concentration (Figures 3H and 3I). Overexpression of *nhr-8* in wild-type animals resulted in higher resistance to *P. aeruginosa* infection compared with control animals only when the animals were grown at 20 μg/mL cholesterol (Figure S8A), indicating that NHR-8 is a rate-limiting factor that mediates the enhanced immunity elicited by high cholesterol.

The cholesterol effect on immune defense required intestinal NHR-8 (Figures 3F, 3G, and 3I), and animals grown on high cholesterol exhibited high expression levels of immune genes (Figures 2B–2D). Therefore, we hypothesized that mutation in *nhr-8* would suppress the upregulation of immune genes induced by high cholesterol. To test this hypothesis, we compared the gene expression of *nhr-8(ok186)* and wild-type animals grown on high cholesterol. We used *pmk-1*-dependent genes (*F55G11.8, C17H12.6, C05A9.1, C32H11.4,* and *R03D7.6*) that are cholesterol dependent (Table S1) and are known markers of innate immune activation in *C. elegans* (Ooi et al., 2012; Troemel et al., 2006). As shown in Figure 4A, *nhr-8* mutation suppressed the upregulation of PMK-1- and DAF-16-dependent genes elicited by high cholesterol. Although NHR-8 seemed to be required for the expression of PMK-1-dependent genes, it did not transcriptionally control *pmk-1* itself (Figure S9). Consistent with the idea that both NHR-8 and PMK-1 are part of the

same immune pathway induced by cholesterol, *nhr-8* and *pmk-1* inactivation had no additive effect on the susceptibility of the animals to *P. aeruginosa*-mediated killing (Figure 4B). We observed no additive effect of inhibition by RNAi of the cholesterol transporter CHUP-1 on *nhr-8(ok186)* animals (Figure S8B), which provides additional support of the idea that NHR-8 is part of the pathway involved in the activation of PMK-1 by cholesterol.

To further substantiate the relationship between NHR-8 and the PMK-1 pathway, we studied whether *nhr-8* mutation could suppress the effect of *vhp-1* RNAi on the susceptibility of the animals to *P. aeruginosa*. VHP-1 inhibition by RNAi is known to promote the activation of PMK-1, which results in enhanced resistance to pathogen infection (Kim et al., 2004; Mizuno et al., 2004). The *nhr-8* mutation suppressed the enhanced resistance to *P. aeruginosa*-mediated killing and the enhanced gene expression of *vhp-1* RNAi animals (Figures 4C and 4D). Taken together, these studies show that cholesterol regulates innate immune defense against *P. aeruginosa* infection via an NHR-8/PMK-1 pathway (Figure 4E).

DISCUSSION

The host immune system fights infecting microbial pathogens through diverse molecular pathways (Akira et al., 2006; Keshet et al., 2017; Sun et al., 2011). The activation and function of these pathways depend on a myriad of genetic, environmental, and nutritional factors. Although the role of cholesterol in various physiological processes in animals is well studied (Ihara et al., 2017; Kawasaki et al., 2013; Magner et al., 2013; Shanmugam et al., 2017), its specific role in the function of the immune system during responses to infections is unknown. In this study, we uncovered the underlying mechanism of the cholesterol requirement for proper innate immune function in *C. elegans*. We further established that the cholesterol transporter CHUP-1 and the nuclear hormone receptor NHR-8 are required for the effect of cholesterol on pathogen resistance. In addition, we provided evidence indicating that cholesterol is required for the activation of immune pathways.

CHUP-1 is evolutionarily conserved, and SIDt1 and SIDt2 are 9-transmembrane domain transporters that are more closely related in humans (Méndez-Acevedo et al., 2017; Valdes et al., 2012; Whangbo et al., 2017). Although SIDTs transport both double-stranded RNA (dsRNA) and cholesterol (Whangbo et al., 2017), dsRNA transport cannot be attained without cholesterol (Valdes et al., 2012). Once inside *C. elegans* cells, cholesterol binds and activates NHR-8 (Motola et al., 2006; Rauthan and Pilon, 2011; Rottiers et al., 2006; Shanmugam et al., 2017; Watts and Ristow, 2017; Wollam et al., 2011; Yoshiyama-Yanagawa et al., 2011), which is also evolutionarily conserved (Hoffmann and Partridge, 2015; Magner et al., 2013; Ménez et al., 2019). Like most NHRs, *nhr-8* is a transcriptional regulator that is involved in steroid biosynthesis and metabolism homeostasis. Consistent with the role of cholesterol in steroid biosynthesis and metabolism, it is not surprising that genes involved in metabolic processes were among the most highly enriched genes, demonstrating altered expression when the animals were grown on different cholesterol concentrations.

Although the relationship between different nutrients and the proper function of the immune system has been studied in *C. elegans* (Komura et al., 2012; Shivers et al., 2009; Wu et al., 2019), the role of cholesterol has not been explored. The present analysis reveals evolutionarily conserved mechanisms that explain the role of cholesterol for proper innate immune activation against invading *P. aeruginosa*, in which a known transporter, CHUP-1, is required for the effect of cholesterol on pathogen resistance. The cholesterol effect on the immune system is mediated by the expression of immune genes that are primarily controlled by the PMK-1 pathway, some of which are also controlled by DAF-16 and SKN-1. The results also indicate that cholesterol activation of PMK-1-dependent gene expression requires NHR-8. The results presented here provide a better understanding of how cholesterol plays a role in the elicitation of innate immunity via conserved pathways that protect the host against pathogenic bacteria.

Limitation of the Study

We performed our initial gene expression analysis using DAVID because it is a widely used tool that, unlike species-specific tools such as WormExp, provides GO terms applicable across all species that in our view facilitates the generation of hypotheses and further studies. A limitation is that the general clusters lack details regarding sub-clusters of genes that may highlight important biological functions. Indeed, our more detailed analysis identified additional pathways that are part of the most highly enriched GO terms. To exclude potential contributions from reproduction, we used L4 animals in our gene expression studies.

Although it is possible that different cholesterol concentrations slightly affect larval development, the animals seem to reach adulthood at the same time. Because we performed the survival studies using adults, we do not believe that any potential difference during larval development would account for the survival differences that we have observed.

METHODS

All methods can be found in the accompanying Transparent Methods supplemental file.

DATA AND CODE AVAILABILITY

RNA sequencing data were deposited in NCBI GEO database under the accession numbers: GSE136881 and GSE137058.

SUPPLEMENTAL INFORMATION

Supplemental Information can be found online at https://doi.org/10.1016/j.isci.2020.101068.

ACKNOWLEDGMENTS

This work was fully supported by NIH grants GM0709077 and AI117911 (to A.A.). Most strains used in this study were obtained from the Caenorhabditis Genetics Center (CGC), which is funded by the NIH Office of Research Infrastructure Programs (P40 OD010440) and the National BioResource Project (NBRP) of Japan. The authors are also grateful to Anne Lespine of INTHERES, Université de Toulouse, INRA, ENVT, Toulouse, France, for providing the *nhr-8(ok186);Pnhr-8::nhr-8::RFP* rescued strain upon request.

AUTHOR CONTRIBUTIONS

B.O and A.A. conceived and designed the experiments. B.O. performed the experiments. B.O. and A.A. analyzed the data and wrote the paper.

DECLARATION OF INTERESTS

The authors declare no competing interests.

Received: November 19, 2019
Revised: March 9, 2020
Accepted: April 13, 2020
Published: May 22, 2020

REFERENCES

Akira, S., Uematsu, S., and Takeuchi, O. (2006). Pathogen recognition and innate immunity. Cell *124*, 783–801.

Angeles-Albores, D., Lee, R.Y., Chan, J., and Sternberg, P.W. (2016). Tissue enrichment analysis for *C. elegans* genomics. BMC Bioinformatics *17*, 366.

Angeles-Albores, D., Lee, R.Y., Chan, J., and Sternberg, P.W. (2018). Two new functions in the wormbase enrichment suite. microPublication Biol. *17*, 1–10.

Antebi, A. (2006). Nuclear hormone receptors in *C. elegans*. WormBook *3*, 1–13.

Antebi, A. (2015). Nuclear receptor signal transduction in *C. elegans*. WormBook *1*, 49.

Bodofsky, S., Koitz, F., and Wightman, B. (2017). Conserved and exapted functions of nuclear receptors in animal development. Nucl. Receptor Res. *4*, 1–41.

Brown, A.L., Liao, Z., and Goodman, M.B. (2008). MEC-2 and MEC-6 in the *Caenorhabditis elegans* sensory mechanotransduction complex: auxiliary subunits that enable channel activity. J. Gen. Physiol. *131*, 605–616.

Calkin, A.C., and Tontonoz, P. (2012). Transcriptional integration of metabolism by the nuclear sterol-activated receptors LXR and FXR. Nat. Rev. Mol. Cel. Biol. *13*, 213.

Chen, Y., Bharill, S., Altun, Z., O'Hagan, R., Coblitz, B., Isacoff, E.Y., and Chalfie, M. (2016). *Caenorhabditis elegans* paraoxonase-like proteins control the functional expression of DEG/ENaC mechanosensory proteins. Mol. Biol. Cell *27*, 1272–1285.

Chen, Y., Panter, B., Hussein, A., Gibbs, K., Ferreira, D., and Allard, P. (2019). BPA interferes with StAR-mediated mitochondrial cholesterol transport to induce germline dysfunctions. Reprod. Toxicol. *90*, 24–32.

Cheong, M.C., Lee, H.-J., Na, K., Joo, H.-J., Avery, L., You, Y.-J., and Paik, Y.-K. (2013). NSBP-1 mediates the effects of cholesterol on insulin/IGF-1 signaling in *Caenorhabditis elegans*. Cell Mol. Life Sci. *70*, 1623–1636.

Cheong, M.C., Na, K., Kim, H., Jeong, S.-K., Joo, H.-J., Chitwood, D.J., and Paik, Y.-K. (2011). A potential biochemical mechanism underlying the influence of sterol deprivation stress on *Caenorhabditis elegans* longevity. J. Biol. Chem. *286*, 7248–7256.

Chitwood, D.J., and Lusby, W.R. (1991). Metabolism of plant sterols by nematodes. Lipids *26*, 619–627.

Chow, Y.-L., Kawasaki, Y., and Sato, F. (2014). Knockdown of the NHR-8 nuclear receptor enhanced sensitivity to the lipid-reducing activity of alkaloids in *Caenorhabditis elegans*. Biosci. Biotechnol. Biochem. *78*, 2008–2013.

Dennis, G., Sherman, B.T., Hosack, D.A., Yang, J., Gao, W., Lane, H.C., and Lempicki, R.A. (2003). DAVID: database for annotation, visualization, and integrated discovery. Genome Biol. *4*, R60.

Evans, E.A., Kawli, T., and Tan, M.-W. (2008). *Pseudomonas aeruginosa* suppresses host immunity by activating the DAF-2 insulin-like signaling pathway in *Caenorhabditis elegans*. PLoS Pathog. *4*, e1000175.

Fischer, M., Regitz, C., Kull, R., Boll, M., and Wenzel, U. (2013). Vitellogenins increase stress resistance of *Caenorhabditis elegans* after *Photorhabdus luminescens* infection depending on the steroid-signaling pathway. Microbes Infect. *15*, 569–578.

Garigan, D., Hsu, A.-L., Fraser, A.G., Kamath, R.S., Ahringer, J., and Kenyon, C. (2002). Genetic analysis of tissue aging in *Caenorhabditis elegans*: a role for heat-shock factor and bacterial proliferation. Genetics *161*, 1101–1112.

Hayes, G.D., Riedel, C.G., and Ruvkun, G. (2011). The *Caenorhabditis elegans* SOMI-1 zinc finger protein and SWI/SNF promote regulation of development by the mir-84 microRNA. Genes Dev. *25*, 2079–2092.

Hieb, W., and Rothstein, M. (1968). Sterol requirement for reproduction of a free-living nematode. Science *160*, 778–780.

Hoffmann, J.M., and Partridge, L. (2015). Nuclear hormone receptors: roles of xenobiotic detoxification and sterol homeostasis in healthy aging. Crit. Rev. Biochem. Mol. Biol. *50*, 380–392.

Houthoofd, K., Braeckman, B.P., Lenaerts, I., Brys, K., De Vreese, A., Van Eygen, S., and Vanfleteren, J.R. (2002). Axenic growth up-regulates mass-specific metabolic rate, stress resistance, and extends life span in *Caenorhabditis elegans*. Exp. Gerontol. *37*, 1371–1378.

Huber, T.B., Schermer, B., Müller, R.U., Höhne, M., Bartram, M., Calixto, A., Hagmann, H., Reinhardt, C., Koos, F., and Kunzelmann, K. (2006). Podocin and MEC-2 bind cholesterol to regulate the activity of associated ion channels. Proc. Natl. Acad. Sci. U S A *103*, 17079–17086.

Ihara, A., Uno, M., Miyatake, K., Honjoh, S., and Nishida, E. (2017). Cholesterol regulates DAF-16 nuclear localization and fasting-induced longevity in *C. elegans*. Exp. Gerontol. *87*, 40–47.

Ikonen, E. (2008). Cellular cholesterol trafficking and compartmentalization. Nat. Rev. Mol. Cell Biol. *9*, 125.

Kamal, M., Moshiri, H., Magomedova, L., Han, D., Nguyen, K.C., Yeo, M., Knox, J., Bagg, R., Won, A.M., and Szlapa, K. (2019). The marginal cells of the *Caenorhabditis elegans* pharynx scavenge cholesterol and other hydrophobic small molecules. Nat. Commun. *10*, 1–16.

Kawasaki, I., Jeong, M.-H., Yun, Y.-J., Shin, Y.-K., and Shim, Y.-H. (2013). Cholesterol-responsive metabolic proteins are required for larval development in *Caenorhabditis elegans*. Mol. Cell *36*, 410–416.

Kerry, S., TeKippe, M., Gaddis, N.C., and Aballay, A. (2006). GATA transcription factor required for immunity to bacterial and fungal pathogens. PLoS One *1*, e77.

Keshet, A., Mertenskötter, A., Winter, S.A., Brinkmann, V., Dölling, R., and Paul, R.J. (2017). PMK-1 p38 MAPK promotes cadmium stress resistance, the expression of SKN-1/Nrf and DAF-16 target genes, and protein biosynthesis in *Caenorhabditis elegans*. Mol. Genet. Genomics *292*, 1341–1361.

Kim, D.H., Liberati, N.T., Mizuno, T., Inoue, H., Hisamoto, N., Matsumoto, K., and Ausubel, F.M. (2004). Integration of *Caenorhabditis elegans* MAPK pathways mediating immunity and stress resistance by MEK-1 MAPK kinase and VHP-1 MAPK phosphatase. Proc. Natl. Acad. Sci. U S A *101*, 10990–10994.

Komura, T., Ikeda, T., Hoshino, K., Shibamura, A., and Nishikawa, Y. (2012). *Caenorhabditis elegans* as an alternative model to study senescence of host defense and the prevention by immunonutrition. In Recent Advances on Model Hosts (Springer), pp. 19–27.

Lee, E.-Y., Shim, Y.-H., Chitwood, D.J., Hwang, S.B., Lee, J., and Paik, Y.-K. (2005). Cholesterol-producing transgenic *Caenorhabditis elegans* lives longer due to newly acquired enhanced stress resistance. Biochem. Biophys. Res. Commun. *328*, 929–936.

Lee, J.-H., Choi, S.-H., Kwon, O.-S., Shin, T.-J., Lee, J.-H., Lee, B.-H., Yoon, I.-S., Pyo, M.K., Rhim, H., and Lim, Y.-H. (2007). Effects of ginsenosides, active ingredients of *Panax ginseng*, on development, growth, and life span of *Caenorhabditis elegans*. Biol. Pharm. Bull. *30*, 2126–2134.

Lee, S.S., and Schroeder, F.C. (2012). Steroids as central regulators of organismal development and lifespan. PLoS Biol. *10*, e1001307.

Lindblom, T.H., and Dodd, A.K. (2006). Xenobiotic detoxification in the nematode *Caenorhabditis elegans*. J. Exp. Zool. A Comp. Exp. Biol. *305*, 720–730.

Magner, D.B., Wollam, J., Shen, Y., Hoppe, C., Li, D., Latza, C., Rottiers, V., Hutter, H., and Antebi, A. (2013). The NHR-8 nuclear receptor regulates cholesterol and bile acid homeostasis in *C. elegans*. Cell Metab. *18*, 212–224.

Mallo, G.V., Kurz, C.L., Couillault, C., Pujol, N., Granjeaud, S., Kohara, Y., and Ewbank, J.J. (2002). Inducible antibacterial defense system in *C. elegans*. Curr. Biol. *12*, 1209–1214.

Matyash, V., Entchev, E.V., Mende, F., Wilsch-Bräuninger, M., Thiele, C., Schmidt, A.W., Knölker, H.-J., Ward, S., and Kurzchalia, T.V. (2004). Sterol-derived hormone (s) controls entry into diapause in *Caenorhabditis elegans* by consecutive activation of DAF-12 and DAF-16. PLoS Biol. *2*, e280.

Méndez-Acevedo, K.M., Valdes, V.J., Asanov, A., and Vaca, L. (2017). A novel family of mammalian transmembrane proteins involved in cholesterol transport. Sci. Rep. *7*, 7450.

Ménez, C., Alberich, M., Courtot, E., Guegnard, F., Blanchard, A., Aguilaniu, H., and Lespine, A. (2019). The transcription factor NHR-8: a new target to increase ivermectin efficacy in nematodes. PLoS Pathog. *15*, e1007598.

Merris, M., Wadsworth, W.G., Khamrai, U., Bittman, R., Chitwood, D.J., and Lenard, J. (2003). Sterol effects and sites of sterol accumulation in *Caenorhabditis elegans* developmental requirement for 4α-methyl sterols. J. Lipid Res. *44*, 172–181.

Mizuno, T., Hisamoto, N., Terada, T., Kondo, T., Adachi, M., Nishida, E., Kim, D.H., Ausubel, F.M., and Matsumoto, K. (2004). The *Caenorhabditis elegans* MAPK phosphatase VHP-1 mediates a novel JNK-like signaling pathway in stress response. EMBO J. *23*, 2226–2234.

Mooijaart, S., Brandt, B., Baldal, E., Pijpe, J., Kuningas, M., Beekman, M., Zwaan, B., Slagboom, P., Westendorp, R., and Van Heemst, D. (2005). *C. elegans* DAF-12, nuclear hormone receptors and human longevity and disease at old age. Ageing Res. Rev. *4*, 351–371.

Motola, D.L., Cummins, C.L., Rottiers, V., Sharma, K.K., Li, T., Li, Y., Suino-Powell, K., Xu, H.E., Auchus, R.J., and Antebi, A. (2006). Identification of ligands for DAF-12 that govern dauer formation and reproduction in *C. elegans*. Cell *124*, 1209–1223.

Ooi, S.-K., Lim, T.-Y., Lee, S.-H., and Nathan, S. (2012). *Burkholderia pseudomallei* kills Caenorhabditis elegans through virulence mechanisms distinct from intestinal lumen colonization. Virulence *3*, 485–496.

Pellegrino, M.W., Nargund, A.M., Kirienko, N.V., Gillis, R., Fiorese, C.J., and Haynes, C.M. (2014). Mitochondrial UPR-regulated innate immunity provides resistance to pathogen infection. Nature *516*, 414.

Piskacek, M., Havelka, M., Jendruchova, K., and Knight, A. (2019). Nuclear hormone receptors: Ancient 9aaTAD and evolutionally gained NCoA activation pathways. J. Steroid Biochem. Mol. Biol. *187*, 118–123.

Prabhu, A.V., Luu, W., Sharpe, L.J., and Brown, A.J. (2016). Cholesterol-mediated degradation of 7-dehydrocholesterol reductase switches the balance from cholesterol to vitamin D synthesis. J. Biol. Chem. *291*, 8363–8373.

Ranawade, A., Mallick, A., and Gupta, B.P. (2018). PRY-1/Axin signaling regulates lipid metabolism in *Caenorhabditis elegans*. PLoS one *13*, e0206540.

Ratnappan, R., Ward, J.D., Yamamoto, K.R., and Ghazi, A. (2016). Nuclear hormone receptors as mediators of metabolic adaptability following reproductive perturbations. In Worm (Taylor & Francis), p. e1151609.

Rauthan, M., and Pilon, M. (2011). The mevalonate pathway in *C. elegans*. Lipids Health Dis. *10*, 243.

Rosenbaum, A.I., Rujoi, M., Huang, A.Y., Du, H., Grabowski, G.A., and Maxfield, F.R. (2009). Chemical screen to reduce sterol accumulation in Niemann–Pick C disease cells identifies novel lysosomal acid lipase inhibitors. Biochim. Biophys. Acta *1791*, 1155–1165.

Rottiers, V., Motola, D.L., Gerisch, B., Cummins, C.L., Nishiwaki, K., Mangelsdorf, D.J., and Antebi, A. (2006). Hormonal control of *C. elegans* dauer formation and life span by a Rieske-like oxygenase. Dev. Cell *10*, 473–482.

Sapir, A., Tsur, A., Koorman, T., Ching, K., Mishra, P., Bardenheier, A., Podolsky, L., Bening-Abu-Shach, U., Boxem, M., and Chou, T.-F. (2014). Controlled sumoylation of the mevalonate pathway enzyme HMGS-1 regulates metabolism during aging. Proc. Natl. Acad. Sci. U S A *111*, E3880–E3889.

Schindler, A.J., Baugh, L.R., and Sherwood, D.R. (2014). Identification of late larval stage developmental checkpoints in *Caenorhabditis elegans* regulated by insulin/IGF and steroid hormone signaling pathways. PLoS Genet. *10*, e1004426.

Shanmugam, G., Mohankumar, A., Kalaiselvi, D., Nivitha, S., Murugesh, E., Shanmughavel, P., and Sundararaj, P. (2017). Diosgenin a phytosterol substitute for cholesterol, prolongs the lifespan and mitigates glucose toxicity via DAF-16/FOXO and GST-4 in *Caenorhabditis elegans*. Biomed. Pharmacother. *95*, 1693–1703.

Shivers, R.P., Kooistra, T., Chu, S.W., Pagano, D.J., and Kim, D.H. (2009). Tissue-specific activities of an immune signaling module regulate physiological responses to pathogenic and nutritional bacteria in *C. elegans*. Cell Host Microbe *6*, 321–330.

Singh, V., and Aballay, A. (2006). Heat-shock transcription factor (HSF)-1 pathway required for *Caenorhabditis elegans* immunity. Proc. Natl. Acad. Sci. U S A *103*, 13092–13097.

Smith, M.M., and Levitan, D.J. (2007). Human NPC1L1 and NPC1 can functionally substitute for the ncr genes to promote reproductive development in *C. elegans*. Biochim. Biophys. Acta *1770*, 1345–1351.

Sun, J., Singh, V., Kajino-Sakamoto, R., and Aballay, A. (2011). Neuronal GPCR controls innate immunity by regulating noncanonical unfolded protein response genes. Science *332*, 729–732.

Sutphin, G.L., and Kaeberlein, M. (2009). Measuring Caenorhabditis elegans life span on solid media. J. Vis. Exp. *27*, e1152.

Sym, M., Basson, M., and Johnson, C. (2000). A model for Niemann–Pick type C disease in the nematode *Caenorhabditis elegans*. Curr. Biol. *10*, 527–530.

Tenor, J.L., and Aballay, A. (2008). A conserved Toll-like receptor is required for *Caenorhabditis elegans* innate immunity. EMBO Rep. *9*, 103–109.

Troemel, E.R., Chu, S.W., Reinke, V., Lee, S.S., Ausubel, F.M., and Kim, D.H. (2006). p38 MAPK regulates expression of immune response genes and contributes to longevity in *C. elegans*. PLoS Genet. *2*, e183.

Valdes, V.J., Athie, A., Salinas, L.S., Navarro, R.E., and Vaca, L. (2012). CUP-1 is a novel protein involved in dietary cholesterol uptake in *Caenorhabditis elegans*. PLoS One *7*, e33962.

Wang, Z., Stoltzfus, J., You, Y.-j., Ranjit, N., Tang, H., Xie, Y., Lok, J.B., Mangelsdorf, D.J., and Kliewer, S.A. (2015). The nuclear receptor DAF-12 regulates nutrient metabolism and reproductive growth in nematodes. PLoS Genet. *11*, e1005027.

Watts, J.L., and Ristow, M. (2017). Lipid and carbohydrate metabolism in *Caenorhabditis elegans*. Genetics *207*, 413–446.

Whangbo, J.S., Weisman, A.S., Chae, J., and Hunter, C.P. (2017). SID-1 domains important for dsRNA import in *Caenorhabditis elegans*. G3 (Bethesda) *7*, 3887–3899.

Wollam, J., Magomedova, L., Magner, D.B., Shen, Y., Rottiers, V., Motola, D.L., Mangelsdorf, D.J., Cummins, C.L., and Antebi, A. (2011). The Rieske oxygenase DAF-36 functions as a cholesterol 7-desaturase in steroidogenic pathways governing longevity. Aging Cell *10*, 879–884.

Wu, Z., Isik, M., Moroz, N., Steinbaugh, M.J., Zhang, P., and Blackwell, T.K. (2019). Dietary restriction extends lifespan through metabolic regulation of innate immunity. Cell Metab. *29*, 1192–1205.e8.

Yang, W., Dierking, K., and Schulenburg, H. (2016). WormExp: a web-based application for a *Caenorhabditis elegans*-specific gene expression enrichment analysis. Bioinformatics *32*, 943–945.

Yoshiyama-Yanagawa, T., Enya, S., Shimada-Niwa, Y., Yaguchi, S., Haramoto, Y., Matsuya, T., Shiomi, K., Sasakura, Y., Takahashi, S., and Asashima, M. (2011). The conserved Rieske oxygenase DAF-36/Neverland is a novel cholesterol-metabolizing enzyme. J. Biol. Chem. *286*, 25756–25762.

Zhang, S., Glukhova, S.A., Caldwell, K.A., and Caldwell, G.A. (2017). NCEH-1 modulates cholesterol metabolism and protects against α-synuclein toxicity in a *C. elegans* model of Parkinson's disease. Hum. Mol. Genet. *26*, 3823–3836.

iScience, Volume *23*

Supplemental Information

Cholesterol Regulates Innate Immunity via Nuclear Hormone Receptor NHR-8

Benson Otarigho and Alejandro Aballay

TRANSPARENT METHODS

Bacterial strains

The bacterial strains used in this study are *Escherichia coli* OP50, *E. coli* HT115(DE3), *Pseudomonas aeruginosa* PA14, and *P. aeruginosa* PA14-GFP. Bacteria were grown in Luria-Bertani (LB) broth at 37°C.

C. elegans strains and growth conditions

Hermaphrodite *C. elegans* (var. Bristol) wild type (N2) was used as the control unless otherwise indicated. The *C. elegans* strains used in this study were CF1038 *daf-16(mu86)*, KU25 *pmk-1(km25), CB75 mec-2(e75)*, RB1645 *c56e6.5(ok2034)*, VC999 *tag-340(ok1496)*, VC2712 *f52f12.7(ok3347)*, RB1919 *W07E6.3(ok2498)*, RB1095 *chup-1(ok1073)*, VC452 *chup-1(gk245),* GR1452 veIs13 *[col-19::GFP + rol-6(su1006)] V. mgEx725 [lin-4::let-7 + ttx-3::*RFP], AA292 *daf-36(k114)*, AE501 *nhr-8(ok186)*, RG1228 *daf-9(rh50)*, DR2281 *daf-9(m540)*, AA1 *daf-12(rh257)*, AA10 *daf-12(rh286)* AA34 *daf-12(rh61)* AA86 *daf-12(rh61rh411)*, MGH171 *alxIs9* [*vha-6p::sid-1::SL2::GFP*], NU3 *dbl-1(nk3)*, KU21 *kgb-1(km21)*, QV225 *skn-1(zj15),* and VC1518 *atf-7(gk715)*, which were obtained from the Caenorhabditis Genetics Center (University of Minnesota, Minneapolis, MN). Other strains that were obtained from National BioResource Project (NBRP) of Japan and used in this work were FX19275 *nhr-8(tm1800)* and FX00599 *ncr-1(tm599)*. The rescued strain; *nhr-8(ok186);Pnhr-8::nhr-8::RFP* was obtained upon request from Anne Lespine of INTHERES, Université de Toulouse, INRA, ENVT, Toulouse, France. The intestine rescued strain, *nhr-8(ok186);Pvha-6::nhr-8* was generated by cloning *nhr-8* DNA downstream *vha-6* promoter. All strains were backcrossed with wild type *C. elegans*.

All strains as well as the control animals were grown at 20^{o}C on nematode growth medium (NGM) plates seeded with *E. coli* OP50 as the food source (Brenner, 1974). Synchronized Animals were grown from eggs to young adults on plates containing different cholesterol concentrations. The recipe for the control NGM plates was as follows: 3 g/L NaCl, 3 g/L peptone, 20 g/L agar, 5 μg/mL cholesterol (Sigma, grade ≥99%), 1 mM MgSO4, 1 mM $CaCl_2$, and 25 mM potassium phosphate buffer (pH 6.0). NGM plates were also prepared using 0 μg/mL (low) and 20 μg/mL (high) cholesterol. In the 0 μg/mL plates, ethanol alone was added while the other components remained the same. No antibiotics were added to the NGM plates except where indicated. While simply omitting cholesterol from NGM pleases provides sub-optimal growing conditions, the complete removal of even trace amounts of sterols by replacing agar with agarose extracted with organic solvents has a

stronger impact on development as it causes the animals to eventually cease to grow and results in a reduce brood size (Merris et al., 2003), (Matyash et al., 2004). Because this can affect the outcome of survival experiments, we decided to use NGM plates with or without cholesterol supplementation.

RNA interference (RNAi)

Knockdown of targeted genes was achieved using RNAi by feeding the animals with *E. coli* strain HT115(DE3) expressing double-stranded RNA (dsRNA) homologous to a target gene (Fraser et al., 2000; Timmons and Fire, 1998). RNAi was carried out according to (Singh and Aballay, 2017; Sun et al., 2011). Briefly, *E. coli* with the appropriate vectors were grown in LB broth containing ampicillin (100 μg/mL) and tetracycline (12.5 μg/mL) at 37°C overnight and plated onto NGM plates containing 100 μg/mL ampicillin and 3 mM isopropyl β-D-thiogalactoside (IPTG) (RNAi plates). RNAi-expressing bacteria were grown at 37°C for 12-14 hours. Gravid adults were transferred to RNAi-expressing bacterial lawns and allowed to lay eggs for 2-3 hours. The gravid adults were removed, and the eggs were allowed to develop at 20°C to young adults for subsequent assays. The RNAi clones were from the Ahringer RNAi library.

C. elegans* survival assay on *Pseudomonas aeruginosa

The *C. elegans* survival assay were carried out on wild-type *P. aeruginosa* strain PA14 lawns that were incubated at 37°C for 12 hours. The survival assay utilized full-lawn bacteria prepared by pipetting 20 μL of 12-hour-cultured *P. aeruginosa* and spreading them completely on the surface of the 3.5-cm-diameter SK plates. The plates were incubated at 37°C for 12 hours and then cooled to room temperature for at least one hour before seeding with synchronized young adult hermaphroditic animals. The SK plates were prepared using 0 μg/mL (low), 5 μg/mL (control), and 20 μg/mL (high) cholesterol. The killing assays were performed at 25°C, and live animals were transferred daily to fresh plates. Animals were scored at the indicated times for survival and transferred to fresh pathogen lawns each day until no progeny were produced. Animals were considered dead when they failed to respond to touch and no pharyngeal pumping was observed. Each experiment was performed in triplicate (n = 60 animals).

Brood size assay

The brood size assay was performed according to (Kenyon et al., 1993; Singh and Aballay, 2017). Ten L4 animals from egg-synchronized populations were transferred to individual plates with corresponding cholesterol conditions (described above) and incubated at 20°C.

The animals were transferred to fresh plates every 24 hours. The progenies were counted and removed daily.

***C. elegans* longevity assays**

Longevity assays were performed on NGM plates containing live- or heat killed-*E. coli* OP50 plates according to (Sun et al., 2011) with the above-described different concentrations of cholesterol. Animals were scored as alive, dead, or gone each day. Animals that failed to display touch-provoked or pharyngeal movement were scored as dead. Experimental groups contained 60 to 100 animals. The assays were performed at 20°C.

Intestinal bacterial load visualization and quantification

Intestinal bacterial loads were visualized and quantified according to (Singh and Aballay, 2017; Singh and Aballay, 2006; Sun et al., 2011). Briefly, *P. aeruginosa*-GFP lawns were prepared as described above. The plates were cooled to ambient temperature for at least one hour before seeding with young gravid adult hermaphroditic animals, and the setup was placed at 25°C for 24 hours. The animals were transferred from *P. aeruginosa*-GFP plates to the center of fresh *E. coli* plates for 10 minutes to eliminate *P. aeruginosa*-GFP on their body. The step was repeated two times more to further eliminate external *P. aeruginosa*-GFP left from earlier steps. Subsequently, ten animals were collected and used for fluorescence imaging to visualize the bacterial load, while another ten animals were transferred into 100 µL of PBS plus 0.01% Triton X-100 and ground. Serial dilutions of the lysates (10^1-10^{10}) were seeded onto LB plates containing 50 µg/mL of kanamycin to select for *P. aeruginosa*-GFP cells and grown overnight at 37°C. Single colonies were counted the next day and represented as the number of bacterial cells or CFU per animal. Three independent experiments were performed for each condition.

***col-19*::GFP visualization and quantification**

GR1452 animals that express GFP at late L4/young adult transition were synchronized and grown in the absence of cholesterol supplementation, 5, and 20 µg/mL cholesterol. Fluorescence imaging of *col-19*::GFP was done using young adult stage (~65 hours post hatching) animals that were grown at 20°C under the different cholesterol concentrations. The fluorescence intensity was quantified using Image J software.

Fluorescence imaging

Fluorescence imaging was carried out according to (Singh and Aballay, 2017; Singh and Aballay, 2006; Sun et al., 2011) with slight modifications. Briefly, animals were anesthetized using an M9 salt solution containing 50 mM sodium azide and mounted onto 2% agar pads. The animals were then visualized for bacterial load using a Leica M165 FC fluorescence

stereomicroscope. Fluorescence was quantified using Fiji-ImageJ (https://imagej.net/Fiji/Downloads).

RNA sequencing and analyses

Approximately 40 gravid animals were placed for 3 hours on 10-cm NGM plates (seeded with *E. coli* OP50) (described above) to obtain a synchronized population, which developed and grew to L4 larval stage at 20ºC. Animals were washed off the plates with M9, frozen in QIAzol using ethanol/dry ice, and stored at -80 prior to RNA extraction. Total RNA was extracted using the RNeasy Plus Universal Kit (Qiagen, Netherlands). Residual genomic DNA was removed using TURBO DNase (Life Technologies, Carlsbad, CA). A total of 6 µg of total RNA was reverse-transcribed with random primers using the High-Capacity cDNA Reverse Transcription Kit (Applied Biosystems, Foster City, CA).

The library construction and RNA sequencing in the BGISEQ-500 platform was performed according to (Yao et al., 2018; Zhu et al., 2018), and paired-end reads of 100 bp were obtained for subsequent data analysis. The RNA sequence data were analyzed using a workflow constructed for Galaxy (https://usegalaxy.org) (Afgan et al., 2018; Afgan et al., 2016; Amrit and Ghazi, 2017). The RNA reads were aligned to the *C. elegans* genome (WS230) using the aligner STAR. Counts were normalized for sequencing depth and RNA composition across all samples. Differential gene expression analysis was then performed using normalized samples. Genes exhibiting at least a two-fold change were considered differentially expressed. The differentially expressed genes were subjected to SimpleMine tools from Wormbase (https://www.wormbase.org/tools/mine/simplemine.cgi) to generate information such as the wormBase ID and gene names, which were employed for further analyses. Gene ontology analysis was performed using the wormBase IDs in DAVID Bioinformatics Database (https://david.ncifcrf.gov) (Dennis et al., 2003) and a *C. elegans* data enrichment analysis tool (https://wormbase.org/tools/enrichment/tea/tea.cgi). The Venn diagrams were obtained using the web tool InteractiVenn (http://www.interactivenn.net) (Heberle et al., 2015) and bioinformatics and evolutionary genomics tool (http://bioinformatics.psb.ugent.be/webtools/Venn/).

RNA isolation and quantitative reverse transcription-PCR (qRT-PCR)

Animals were synchronized, and total RNA extraction was performed following the above-described protocol. qRT-PCR was conducted using the Applied Biosystems One-Step Real-time PCR protocol using SYBR Green fluorescence (Applied Biosystems) on an Applied Biosystems 7900HT real-time PCR machine in 96-well-plate format. Twenty-five-microliter reactions were analyzed as outlined by the manufacturer (Applied Biosystems). The relative

fold changes of the transcripts were calculated using the comparative $CT(2^{-\Delta\Delta CT})$ method and normalized to pan-actin (*act-1, -3, -4*). The cycle thresholds of the amplification were determined using StepOnePlus™ Real-Time PCR System Software v2.3 (Applied Biosystems). All samples were run in triplicate. The primer sequences are available upon request and are presented in Table S6.

Generation of transgenic *C. elegans*

The *nhr-8* DNA was amplified from genomic DNA of Bristol N2 *C. elegans* adult worms as template using the primers presented in Table S6. Linearization of plasmid pPD95.77_Pvha-6_SL2 was performed by restriction digestion using SalI and SmaI enzymes. The amplified nhr-8 DNA was cloned under the vha-6 promoter in plasmid pPD95.77*_Pvha-6_*SL2 between the SalI and SmaI sites to generate the expression clone pPD95.77*_Pvha-6_nhr-8*_SL2. The construct was purified and sequenced. Young adult hermaphrodite *nhr-8(ok186) C. elegans* were transformed by microinjection of plasmids into the gonads according to (Mello and Fire, 1995; Mello et al., 1991). A mixture containing the pPD95.77*_Pvha-6_nhr-8*_SL2 plasmids (40 ng/µL) and pRF4_ *rol-6(su1006)* (10 ng/µL) as a transformation marker was injected into the worm. Successful transformation was determined by identification of the selection marker as dominant roller. At least three independent lines carrying extra chromosomal arrays were obtained for each construct. Only worms with dominant roller were selected for further experiments.

Western blot analysis

Whole-worm lysates of L4 stage grown at 5 and 20 µg/mL cholesterol were prepared according to (Cao and Aballay, 2016). Phosphorylated PMK-1 protein was detected using an anti-active p38 polyclonal antibody from rabbit (1:2000, Promega) and β-actin was detected using a monoclonal anti-actin antibody from mouse (1:1000, Abcam).

Quantification and statistical analysis

Statistical analysis was performed with Prism 8 version 8.1.2 (GraphPad). All error bars represent the standard deviation (SD). The two-sample t test was used when needed, and the data were judged to be statistically significant when $p < 0.05$. In the figures, asterisks (*) denote statistical significance as follows: *, $p < 0.05$, **, $p < 0.001$, ***, $p < 0.0001$, as compared with the appropriate controls. The Kaplan-Meier method was used to calculate the survival fractions, and statistical significance between survival curves was determined using the log-rank test. All experiments were performed in triplicate.

Supplemental References

Afgan, E., Baker, D., Batut, B., Van Den Beek, M., Bouvier, D., Čech, M., Chilton, J., Clements, D., Coraor, N., and Grüning, B.A. (2018). The Galaxy platform for accessible, reproducible and collaborative biomedical analyses: 2018 update. Nucleic acids research *46*, W537-W544.

Afgan, E., Baker, D., Van den Beek, M., Blankenberg, D., Bouvier, D., Čech, M., Chilton, J., Clements, D., Coraor, N., and Eberhard, C. (2016). The Galaxy platform for accessible, reproducible and collaborative biomedical analyses: 2016 update. Nucleic acids research *44*, W3-W10.

Amrit, F.R., and Ghazi, A. (2017). Transcriptomic Analysis of C. elegans RNA Sequencing Data Through the Tuxedo Suite on the Galaxy Project. JoVE (Journal of Visualized Experiments), e55473.

Cao, X., and Aballay, A. (2016). Neural inhibition of dopaminergic signaling enhances immunity in a cell-non-autonomous manner. Current Biology *26*, 2329-2334.

Dennis, G., Sherman, B.T., Hosack, D.A., Yang, J., Gao, W., Lane, H.C., and Lempicki, R.A. (2003). DAVID: database for annotation, visualization, and integrated discovery. Genome biology *4*, R60.

Fraser, A.G., Kamath, R.S., Zipperlen, P., Martinez-Campos, M., Sohrmann, M., and Ahringer, J. (2000). Functional genomic analysis of *C. elegans* chromosome I by systematic RNA interference. Nature *408*, 325.

Heberle, H., Meirelles, G.V., da Silva, F.R., Telles, G.P., and Minghim, R. (2015). InteractiVenn: a web-based tool for the analysis of sets through Venn diagrams. BMC bioinformatics *16*, 169.

Kenyon, C., Chang, J., Gensch, E., Rudner, A., and Tabtiang, R. (1993). A *C. elegans* mutant that lives twice as long as wild type. Nature *366*, 461.

Matyash, V., Entchev, E.V., Mende, F., Wilsch-Bräuninger, M., Thiele, C., Schmidt, A.W., Knölker, H.-J., Ward, S., and Kurzchalia, T.V. (2004). Sterol-derived hormone (s) controls entry into diapause in *Caenorhabditis elegans* by consecutive activation of DAF-12 and DAF-16. PLoS biology *2*, e280.

Mello, C., and Fire, A. (1995). DNA transformation. In Methods in cell biology (Elsevier), pp. 451-482.

Mello, C.C., Kramer, J.M., Stinchcomb, D., and Ambros, V. (1991). Efficient gene transfer in C. elegans: extrachromosomal maintenance and integration of transforming sequences. The EMBO journal *10*, 3959-3970.

Merris, M., Wadsworth, W.G., Khamrai, U., Bittman, R., Chitwood, D.J., and Lenard, J. (2003). Sterol effects and sites of sterol accumulation in *Caenorhabditis elegans* developmental requirement for 4α-methyl sterols. Journal of lipid research *44*, 172-181.

Singh, J., and Aballay, A. (2017). Endoplasmic reticulum stress caused by lipoprotein accumulation suppresses immunity against bacterial pathogens and contributes to immunosenescence. MBio *8*, e00778-00717.

Singh, V., and Aballay, A. (2006). Heat-shock transcription factor (HSF)-1 pathway required for *Caenorhabditis elegans* immunity. Proceedings of the National Academy of Sciences *103*, 13092-13097.

Sun, J., Singh, V., Kajino-Sakamoto, R., and Aballay, A. (2011). Neuronal GPCR controls innate immunity by regulating noncanonical unfolded protein response genes. Science *332*, 729-732.

Timmons, L., and Fire, A. (1998). Specific interference by ingested dsRNA. Nature *395*, 854.

Yao, L., Wang, J., Li, B., Meng, Y., Ma, X., Si, E., Ren, P., Yang, K., Shang, X., and Wang, H. (2018). Transcriptome sequencing and comparative analysis of differentially-expressed isoforms in the roots of Halogeton glomeratus under salt stress. Gene *646*, 159-168.

Zhu, F.-Y., Chen, M.-X., Ye, N.-H., Qiao, W.-M., Gao, B., Law, W.-K., Tian, Y., Zhang, D., Zhang, D., and Liu, T.-Y. (2018). Comparative performance of the BGISEQ-500 and Illumina HiSeq4000 sequencing platforms for transcriptome analysis in plants. Plant methods *14*, 69.

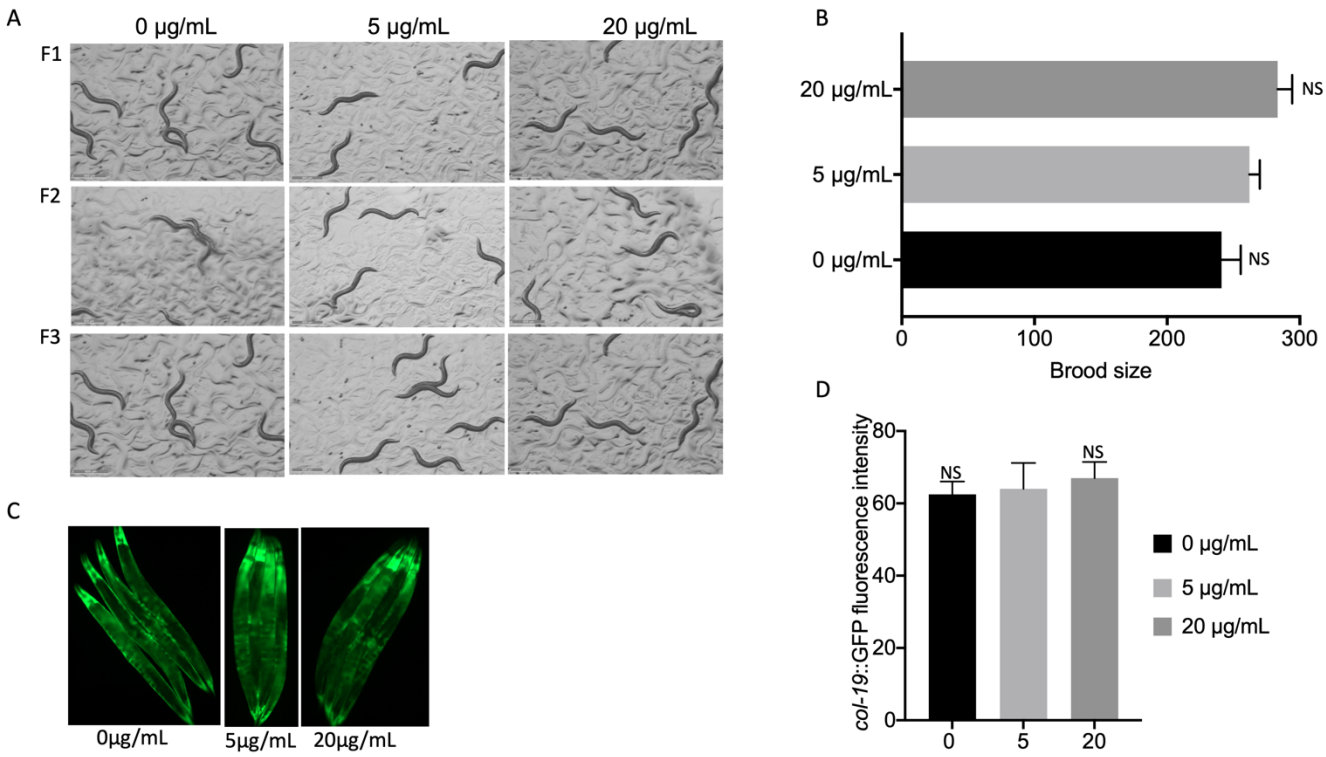

Figure S1. The absence of cholesterol supplementation does not affect the development or brood size of *C. elegans.* Related to Figure 1.

(A) Microscopic images of animals grown in the absence and different cholesterol supplementation concentrations for three generations. Microscopic images were obtained at the young adult stage (~65 hours post hatching).

(B) Brood size of animals grown in the absence and different cholesterol concentrations. Bars represent means while error bars indicate SD; P = NS.

(C) Fluorescence images of GR1452 young adult animals (expressing GFP) grown in the absence of cholesterol supplementation and at different cholesterol concentrations. Microscopic images were obtained at the young adult stage (~65 hours post hatching).

(D) Quantification of *col-19*::GFP expression of GR1452 animals grown in the absence of cholesterol supplementation and at different cholesterol concentrations. Fluorescence was quantified using Fiji-ImageJ. Bars represent means while error bars indicate SD; P = NS.

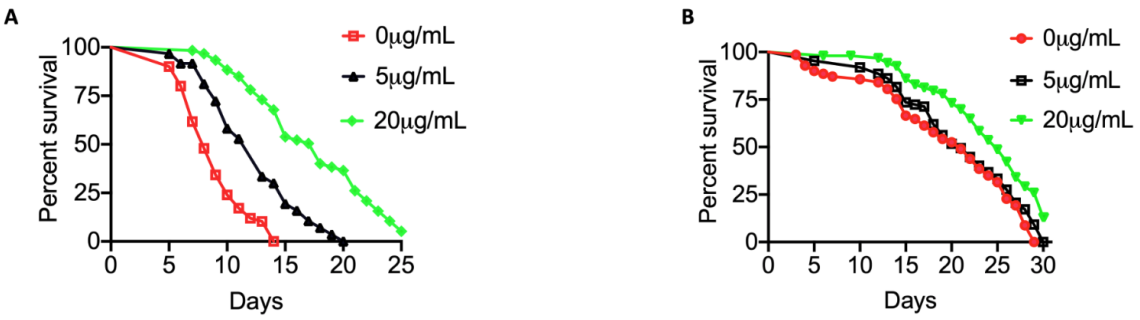

Figure S2. Lifespan of the *C elegans* grown on different cholesterol concentrations on live and heat-killed *E. coli*. Related to Figure 1.

(A) Survival of WT animals grown on *E. coli* at different cholesterol concentrations, transferred to live *E. coli* cultured at the control cholesterol concentration (5 μg/mL), and scored for survival. WT animals on live *E. coli* 5 μg/mL vs. 0 μg/mL, $P < 0.0001$; 20 μg/mL, $P < 0.0001$.

(B) Survival of WT animals grown on *E. coli* at different cholesterol concentrations, transferred to heat-killed *E. coli* seeded on plates with control cholesterol concentration (5 μg/mL) and 50 μg/mL streptomycin, and scored for survival. WT animals on heat-killed *E. coli* 5 μg/mL vs. 0 μg/mL, P = NS; 20 μg/mL, $P < 0.001$.

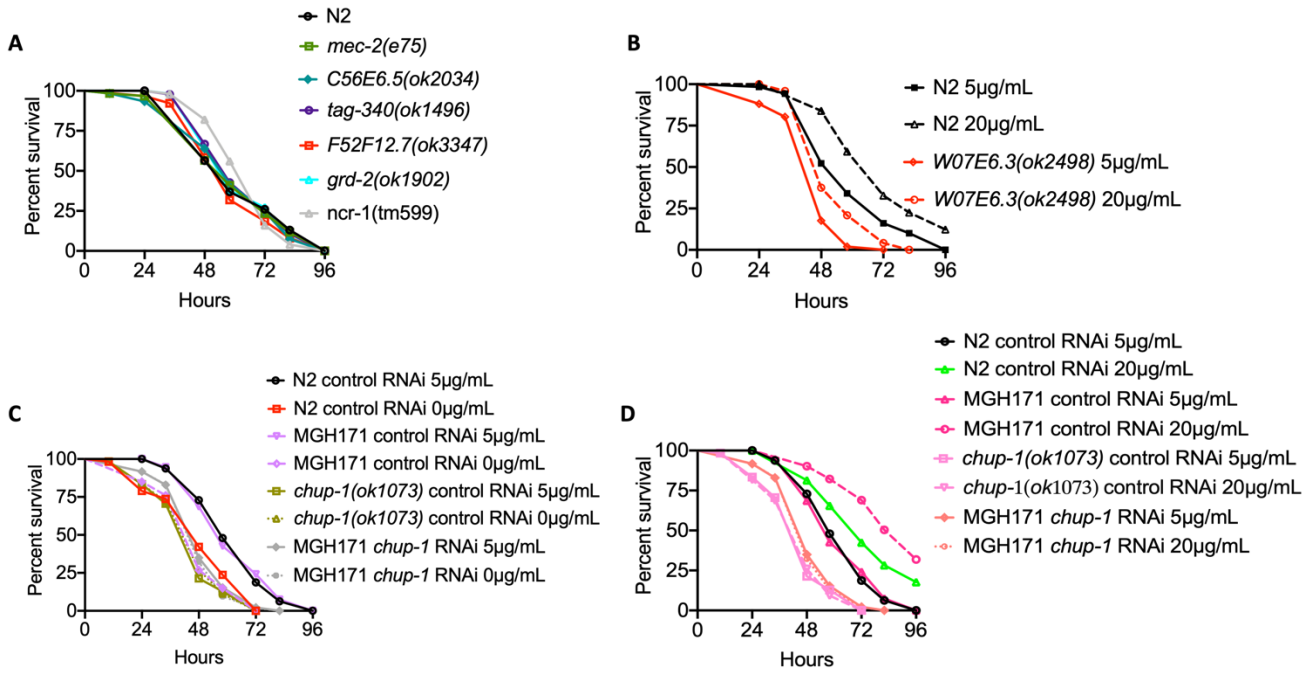

Figure S3. Survival of animals deficient in cholesterol transporters infected with *P. aeruginosa*. Related to Figure 1.

(A) WT animals and mutants in cholesterol transporters were grown on 5µg/mL cholesterol, exposed to *P. aeruginosa,* and scored for survival. WT animal vs. cholesterol transporter loss-of-function animals, P = NS.

(B) WT animals and *W07E6.3(ok2498)* were grown on 5 and 20 µg/mL cholesterol, exposed to *P. aeruginosa*, and scored for survival. *W07E6.3(ok2498)* grown on 5µg/mL cholesterol vs. 20 µg/mL cholesterol, P < 0.001

(C) Control, MGH171(*chup-1* RNAi), WT (*chup-1* RNAi), and *chup-1(ok1073)* RNAi animals were grown on were 0 and 5µg/mL cholesterol, exposed to *P. aeruginosa,* and scored for survival. MGH171 *chup-1* RNAi grown on 5µg/mL cholesterol vs. MGH171 *chup-1* RNAi grown on 0µg/mL, P = NS.

(D) Control, MGH171(*chup-1* RNAi), WT (*chup-1* RNAi), and *chup-1(ok1073)* RNAi animals were grown on were 20 and 5µg/mL cholesterol, exposed to *P. aeruginosa,* and scored for survival. MGH171 *chup-1* RNAi grown on 5µg/mL cholesterol vs. MGH171 *chup-1* RNAi grown on 20µg/mL, P = NS.

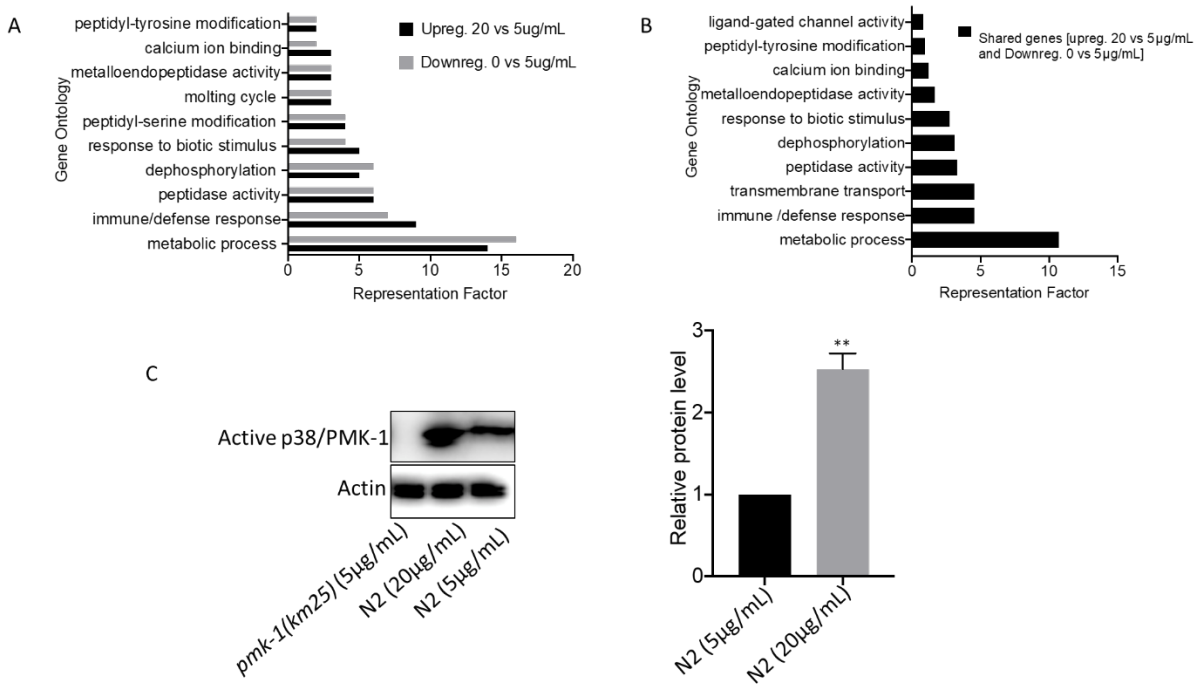

Figure S4: Analysis of cholesterol genes and active PMK-1/p38 levels. Related to Figures 2 and 4.

(A) Enrichment analysis of upregulated genes at 20 vs 5 µg/mL and downregulated genes at 0 vs 5 µg/mL cholesterol. The cutoff is based on the filtering thresholds of $P < 0.05$ and arranged according to the representation factor.

(B) Enrichment analysis of shared genes between animals grown at 20 vs. 5 µg/mL and 0 vs. 5 µg/mL cholesterol. The cutoff is based on the filtering thresholds of $P < 0.05$ and arranged according to the representation factor.

(C) Western blot analysis of active PMK-1/p38 levels in wild-type animals grown at different cholesterol concentration. Image quantification was performed using the software program Fiji/ImageJ. Bars represent means while error bar indicates SD; $**p < 0.001$

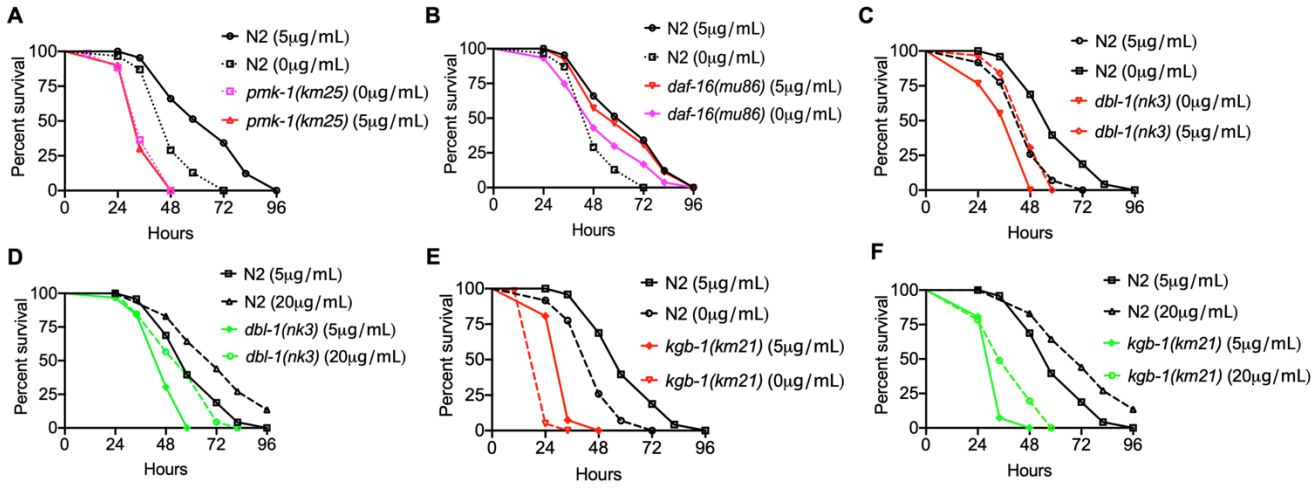

Figure S5. Survival of mutants in immune genes grown at different cholesterol concentrations. Related to Figure 2.

(A) WT and *pmk-1(km25)* animals were grown on 0 and 5 µg/mL cholesterol, exposed to *P. aeruginosa,* and scored for survival. WT animals grown on 5µg/mL cholesterol (control) vs. 0µg/mL, P< 0.0001; *pmk-1(km25)* 0µg/mL, P< 0.0001; *pmk-1(km25)* 5µg/mL, P= P>0.0001. *pmk-1(km25)* 0µg/mL vs. *pmk-1(km25)* 5µg/mL, P=NS.

(B) WT and *daf-16(mu86)* animals were grown on 0 and 5 µg/mL cholesterol, exposed to *P. aeruginosa,* and scored for survival. WT animals grown on 5µg/mL cholesterol (control) vs. 0µg/mL, P< 0.0001; *daf-16(mu86)* 0µg/mL, P< 0.0001; *daf-16(mu86)* 5µg/mL, P= NS.

(C) WT and *dbl-1(nk3)* animals were grown on 0 and 5µg/mL cholesterol, exposed to *P. aeruginosa,* and scored for survival. *dbl-1(nk3)* animals grown on 5 µg/mL cholesterol (control) vs. 0 µg/mL, P< 0.001.

(D) WT and *dbl-1(nk3)* animals were grown on 20 and 5µg/mL cholesterol, exposed to *P. aeruginosa,* and scored for survival. *dbl-1(nk3)* animals grown on 5µg/mL cholesterol (control) vs. 20, P< 0.001.

(E) WT and *kgb-1(km21)* animals were grown on 0 and 5µg/mL cholesterol, exposed to *P. aeruginosa,* and scored for survival. *kgb-1(km21)* animals grown on 5µg/mL cholesterol (control) vs. 0, P< 0.001.

(F) WT and *kgb-1(km21)* animals were grown on 20 and 5µg/mL cholesterol, exposed to *P. aeruginosa,* and scored for survival. *kgb-1(km21)* animals grown on 5µg/mL cholesterol (control) vs. 20, P< 0.001.

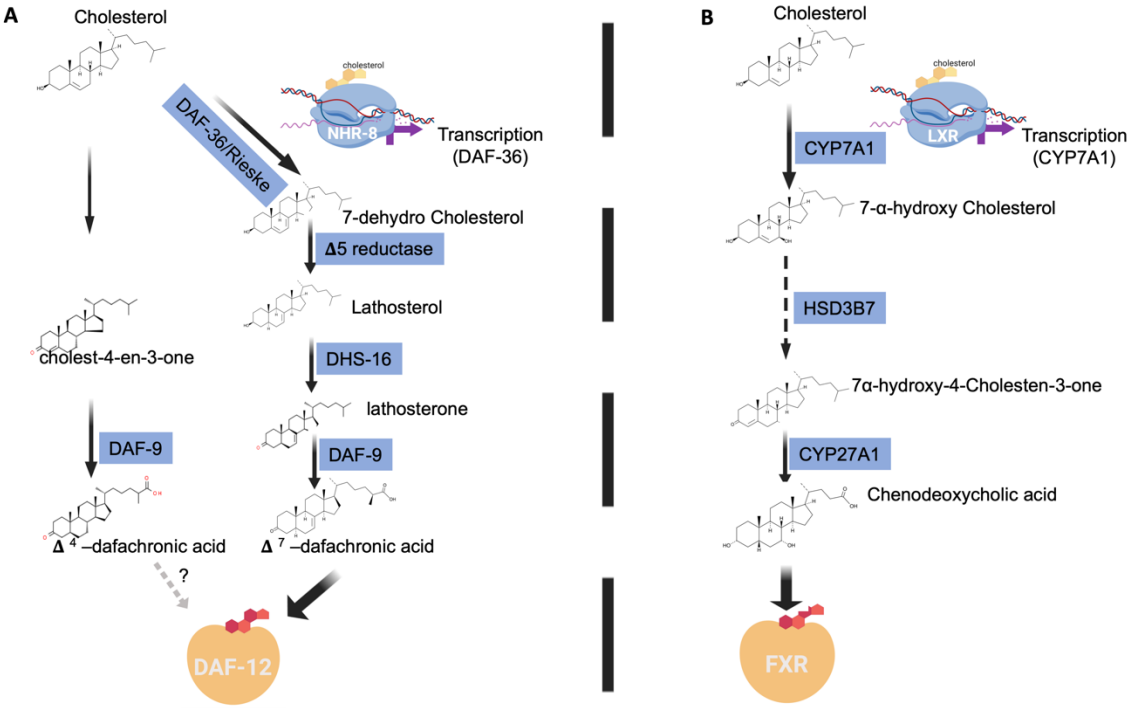

Figure S6. Diagram of the steroid biosynthesis pathways. Related to Figure 3.
(A) *C. elegans* and (B) mammalian steps and genes are shown purple color.
Modified from: Antebi, A., 2015. Nuclear receptor signal transduction in *C. elegans*. WormBook, 1, p.49.

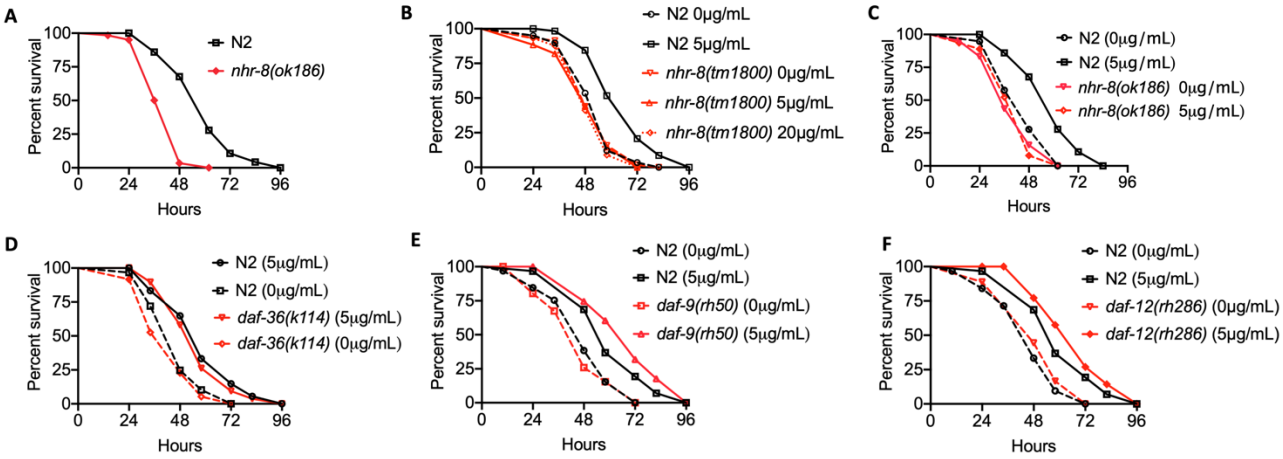

Figure S7. Survival of mutants in genes required for steroid synthesis grown at different cholesterol concentrations. Related to Figure 3

(A) WT and *nhr-8(ok186)* animals were grown on 5 µg/mL cholesterol, exposed to *P. aeruginosa,* and scored for survival. WT animals vs. *nhr-8(ok186)*, P < 0.0001.

(B) WT and *nhr-8(tm1800)* animals were grown on 0, 5 and 20 µg/mL cholesterol supplementation, exposed to *P. aeruginosa,* and scored for survival. WT animals vs. *nhr-8(tm1800)*, P < 0.001; *8(tm1800)* at 5 µg/mL vs. *8(tm1800)* at 0 µg/mL, P = NS; vs *8(tm1800)* at 20 µg/mL, P= NS.

(C) WT and *nhr-8(ok186)* animals were grown on 0 and 5µg/mL cholesterol, exposed to *P. aeruginosa,* and scored for survival. WT animals grown on 5µg/mL cholesterol (control) vs. WT animals 0µg/mL, P< 0.0001; *nhr-8(ok186)* 0µg/mL, P< 0.0001; *nhr-8(ok186)* 5µg/mL,

(D) WT and *daf-36(k114)* animals were grown on 0 and 5µg/mL cholesterol, exposed to *P. aeruginosa,* and scored for survival. WT animals grown on 5µg/mL cholesterol (control) vs. WT animals 0µg/mL, P< 0.0001; *daf-36(k114)* 0µg/mL, P< 0.0001; *daf-36(k114)* 5µg/mL, P = NS. *daf-36(k114)* animals on 0µg/mL vs. *daf-36(k114)* 5µg/mL, P< 0.0001.

(E) WT and *daf-9(rh50)* animals were grown on 0 and 5µg/mL cholesterol, exposed to *P. aeruginosa,* and scored for survival. WT animals grown on 5µg/mL cholesterol (control) vs. WT animals 0µg/mL, P< 0.0001; *daf-9(rh50)* 0µg/mL, P< 0.0001; *daf-9(rh50)* 5µg/mL, P < 0.001. *daf-9(rh50)* animals on 0µg/mL vs. *daf-9(rh50)* 5µg/mL, P< 0.0001.
P< 0.0001. *nhr-8(ok186)* animals on 0µg/mL vs. *nhr-8(ok186)* 5µg/mL, P=NS.

(F) WT and *daf-12(rh286)* animals were grown on 0 and 5µg/mL cholesterol, exposed to *P. aeruginosa,* and scored for survival. WT animals grown on 5µg/mL cholesterol (control) vs. WT animals on 0µg/mL, P< 0.0001; *daf-12(rh286)* 0µg/mL, P< 0.0001; *daf-12(rh286)* 5µg/mL, P< 0.001. *daf-12(rh286)* mutant on 0µg/mL vs. *daf-12(rh286)* 5µg/mL, P< 0.0001.

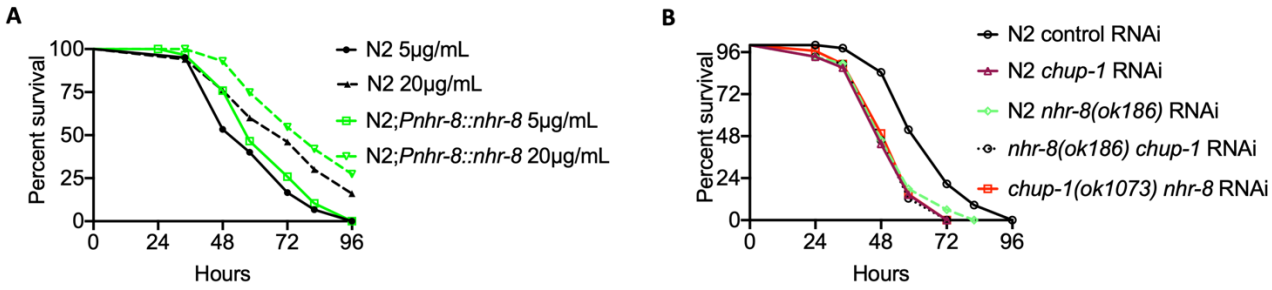

Figure S8: NHR-8 and CHUP-1 are part of the same pathway that promotes cholesterol-mediated innate immunity . Related to Figure 3

(A) WT;*Pnhr-8::nhr-8* animals were grown in the absence of cholesterol supplementation and at 5µg/mL cholesterol, exposed to *P. aeruginosa,* and scored for survival. WT animals grown on 20µg/mL cholesterol (control) vs. WT;*Pnhr-8::nhr-8* at 20µg/mL, P<0.001.
(B) Control RNAi on WT, *chup-1(ok1013),* and *nhr-8(186)* alongside with *chup-1* RNAi on *nhr-8(186)* animals were grown on 5 µg/mL cholesterol, exposed to *P. aeruginosa*, and scored for survival. *nhr-8(186)* (chup-1 RNAi) vs. *chup-1(ok1013)*(control RNAi), P=NS; vs. *nhr-8(186)* (control RNAi), P=NS.

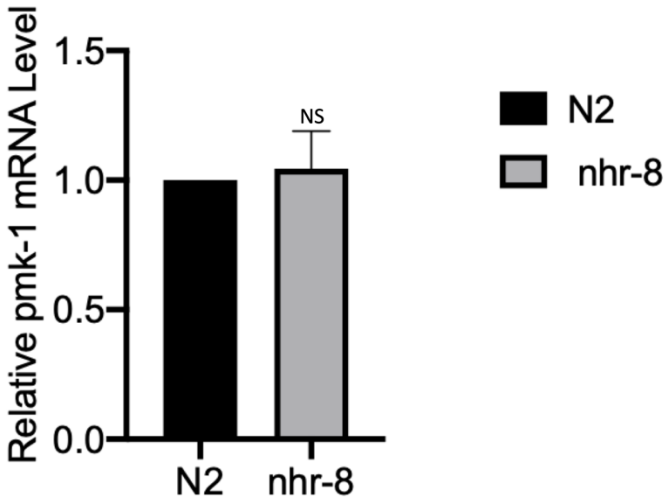

Figure S9. *pmk-1* expression in N2 and *nhr-8(ok186)* animals. Related to Figure 4.
Gene expression of *pmk-1* in *nhr-8(ok186)* and N2 animals grown on 5 μg/mL cholesterol on *E. coli*. Bars represent means while error bar indicates SD; P=NS